INAF

ISTITUTO NAZIONALE DI ASTROFISICA
OSSERVATORIO ASTROFISICO DI ARCETRI

UNIVERSITÀ DEGLI STUDI FIRENZE

Lecture IV:
The Spectral Energy Distribution of Galaxies
Stellar population properties from optical/NIR light

Astrophysics of Galaxies 2019-2020

Stefano Zibetti - INAF Osservatorio Astrofisico di Arcetri

Lecture IV

Objectives

- How many stars? Better, how much stellar mass?
  Key for:
  - scaling relations
  - dynamics
- When did stars form? ***Age!***
- What is their chemical composition? ***Metallicity and beyond***
- and how is it related to their age? ***Age-metallicity distributions***
- Can we reconstruct the full star-formation and chemical enrichment history?

Methods

- Compare ***observed*** starlight to (complex) ***models*** of starlight from stellar population synthesis (SPS)
- Models:
  - Simple Stellar Populations (see lecture III)
  - add complexity - complex star-formation and chemical-enrichment histories
  - add more complexity - dust
  - add even more complexity - variable IMF
- Observations: choose the right dataset — maximise information, minimise noise and sensitivity to model uncertainties
- Statistical methods for inference

Best case: observe individual stars

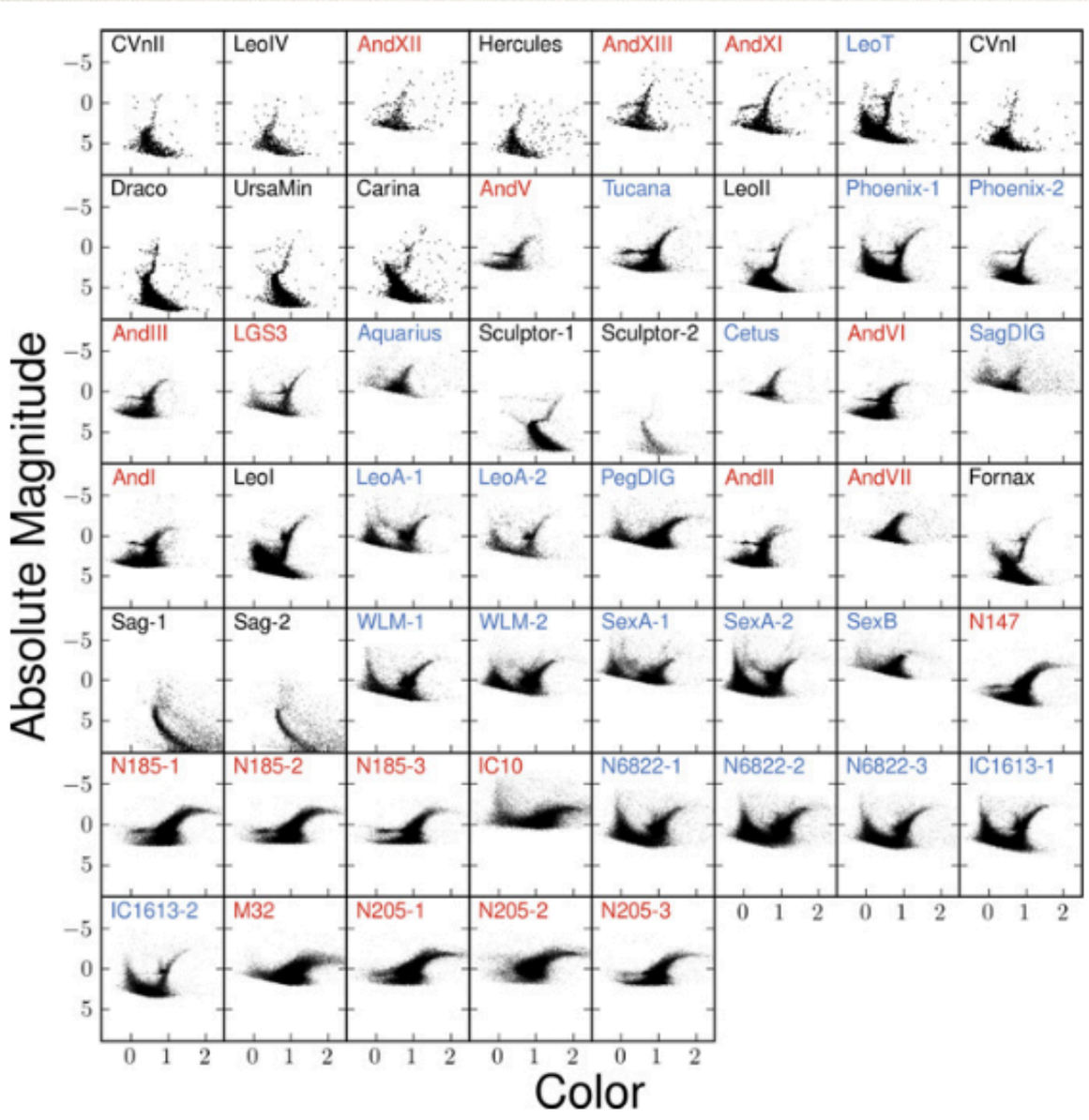

Figure 3. CMDs of all fields analyzed in this paper, sorted by the increasing absolute *V*-band magnitude. The field names are color-coded by a galaxy's association with the MW (black), M31 (red), or the field (blue). Given the heterogeneity in filter sets, we have indicated only a canonical color and reddest available magnitude on the *x* and *y* axes, respectively. The specific filter combinations are listed in Table 2. All galaxies associated with the MW have CMDs that extend below the oldest MSTO. However, only two field galaxies (Phoenix and Leo T) and no galaxies associated with M31 have comparably deep CMDs.

Weisz et al. (2014)

- Build observed CMDs and find the best-fitting combination of SSPs that reproduce the observations.
- The weight of each SSP as a function of age gives the star-formation history of the galaxy

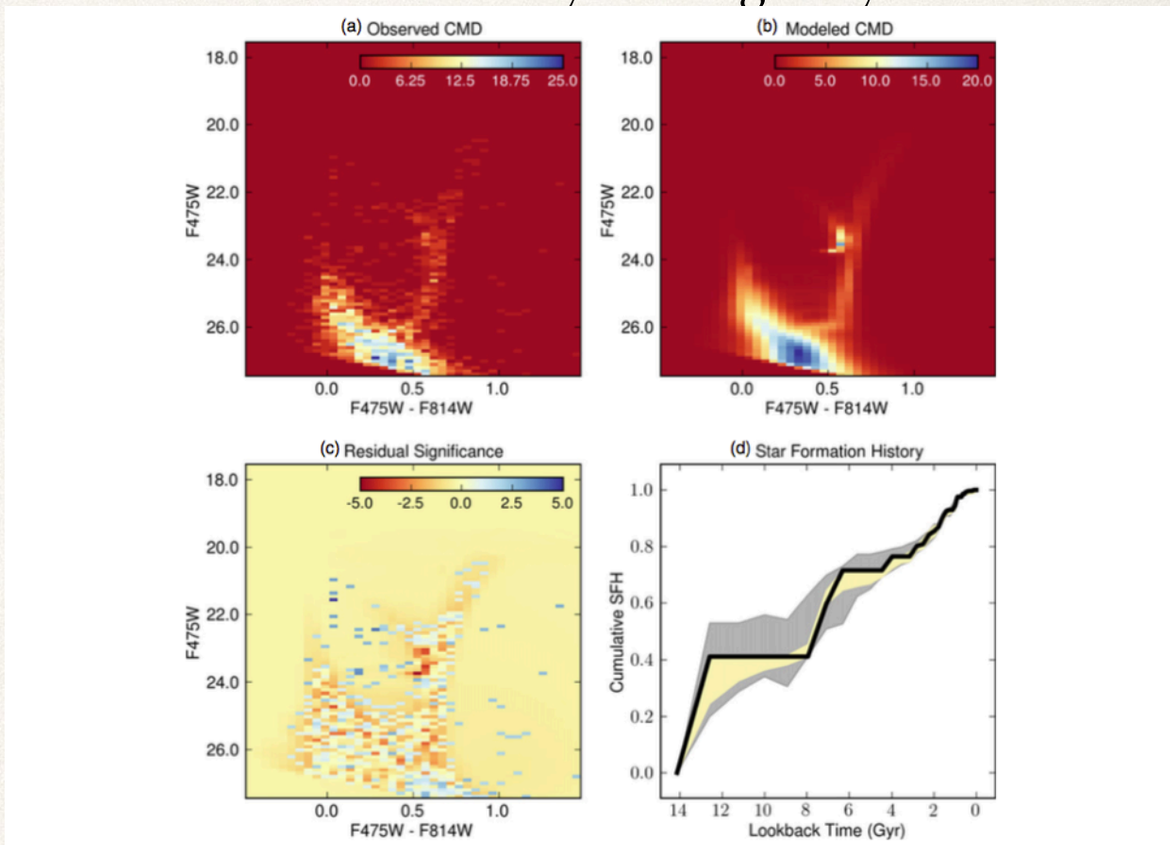

Figure 4. Illustration of the SFH fitting process using Leo T. (a) The observed Hess diagram; (b) best fit model Hess diagram; (c) residual significance Hess diagram; (d) the cumulative SFH, i.e., fraction of the total stellar mass formed prior to a given epoch. In panels (a) and (b) the color-scale reflects the number of stars. In panel (c) the scaling reflects the significance of each pixel in the residual relative to the standard deviation of a Poisson distribution. In panel (d) the best fit SFH is the solid black line and the error envelopes represent the 68% confidence interval around the best fit due to random (yellow) and total (random and systematic; gray) uncertainties. Overall, the best fit model does an excellent job of reproducing the observed Hess diagram of Leo T, as indicated by the lack of strong coherent structure in the panel (c). The process of SFH measurement and uncertainty analysis is discussed in Section 3.

- Only possible for Local Group galaxies using HST
- Future: 30m-class telescopes (ELT, TMT) will extend this to a range of several Mpc
- Otherwise, we must use integrated light

Composite stellar populations

- Star formation history (SFH): star-formation rate $SFR(t) \equiv \frac{dM^*}{dt}$
- In the simplest case, a given SFR at time t and integrated for a time dt results in a SSP of total mass $dM^* = SFR(t)\, dt$ and age t_{obs}-t
- *In* general, at each time we should consider a superposition of SSPs with different chemical enrichment and different dust attenuation
- Let's now follow the time evolution of the flux emitted by a composite stellar population (CSP) from its birth ($t=0$) on…

Composite Stellar Populations

$$f_{\rm CSP}(t) = \int_{t'=0}^{t'=t} \mathrm{SFR}(t-t') \quad f_{\rm SSP}(t', Z) \quad \mathrm{d}t'$$

- Linear superposition of more SSPs according to a star formation history dM(t)=SFR(t-t') dt'

Composite Stellar Populations

$$f_{\rm CSP}(t) = \int_{t'=0}^{t'=t} \int_{Z=0}^{Z_{\rm max}} \Big({\rm SFR}(t-t')\, P(Z, t-t')\, f_{\rm SSP}(t', Z) \Big)\, {\rm d}t'\, {\rm d}Z$$

- Linear superposition of more SSPs according to a star formation history dM(t)=SFR(t-t') dt'

- (Time-dependent) variable metallicity

Composite Stellar Populations

$$f_{\rm CSP}(t) = \int_{t'=0}^{t'=t} \int_{Z=0}^{Z_{\rm max}} \Big({\rm SFR}(t-t')\, P(Z, t-t')\, f_{\rm SSP}(t', Z)\, e^{-\tau_d(t')} \Big)\, {\rm d}t'\, {\rm d}Z$$

- Linear superposition of more SSPs according to a star formation history dM(t)=SFR(t-t') dt'
- (Time-dependent) variable metallicity
- (Time-dependent) dust attenuation

Composite Stellar Populations

$$f_{\rm CSP}(t) = \int_{t'=0}^{t'=t} \int_{Z=0}^{Z_{\rm max}} \left({\rm SFR}(t-t')\, P(Z, t-t')\, f_{\rm SSP}(t', Z)\, e^{-\tau_d(t')} + A\, f_{\rm dust}(t', Z) \right) {\rm d}t'\, {\rm d}Z$$

- Linear superposition of more SSPs according to a star formation history dM(t)=SFR(t-t') dt'
- (Time-dependent) variable metallicity
- (Time-dependent) dust attenuation
- "Contamination" by dust emission (time- and Z-dependent) and nebular emission...

Examples of (non-parametric) CSP

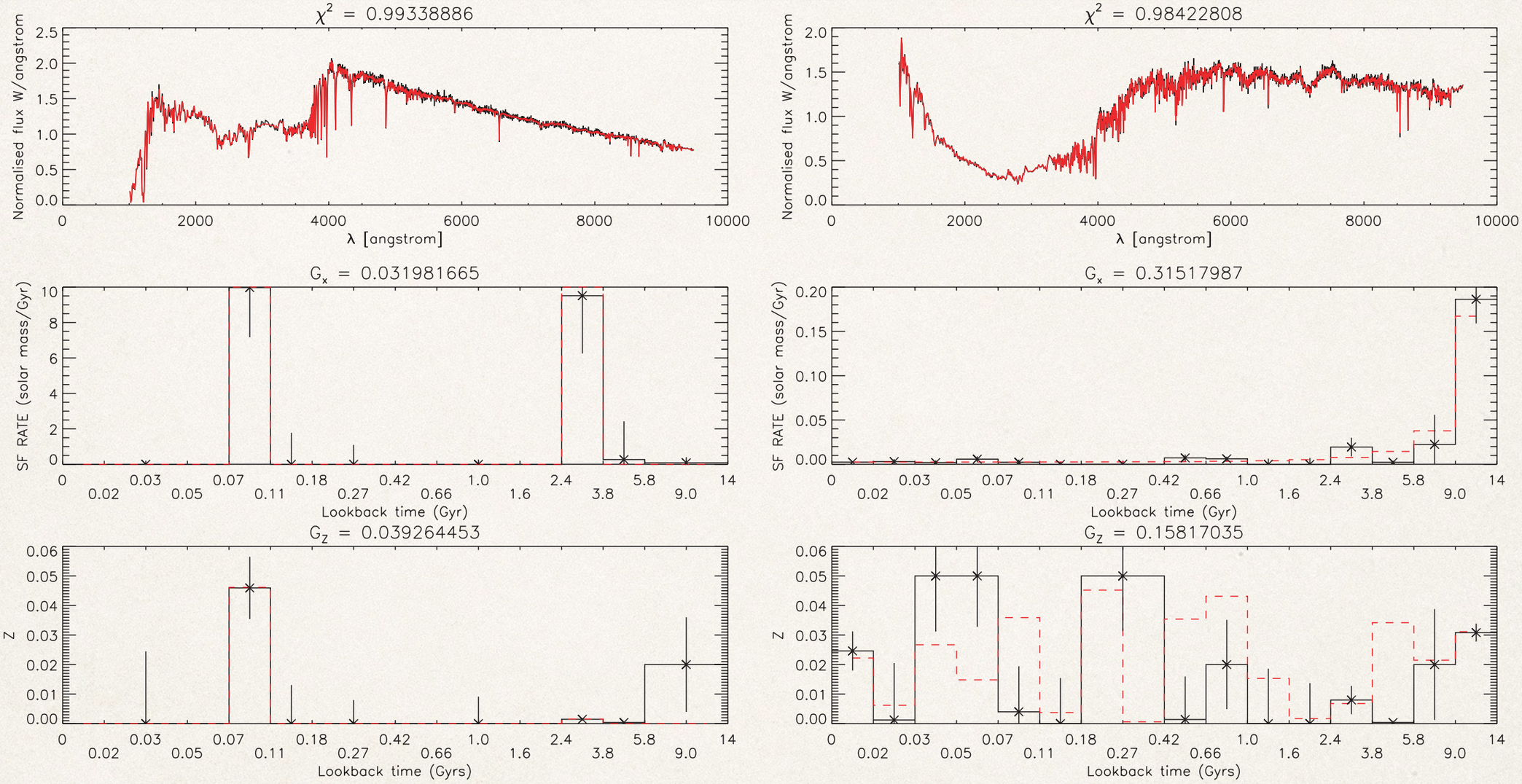

Figure 4. Two examples of VESPA's analysis on synthetic galaxies. The top panels show the original spectrum in the dark line (black in the online version) and fitted spectrum in the lighter line (red in the online version). The middle panels show the input (dashed, red) and the recovered (solid, black) SFRs and the bottom panel shows the input (dashed, red) and recovered (solid, black) metallicities per bin. Note that even though many of the recovered metallicities are wrong, these tend to correspond to bins with very little star formation, and are therefore virtually unconstrained.

Tojeiro et al. (2007)

Popular SFH parameterizations

- SSP $SFR(t)=\delta_{Dirac}(t)$
- Falling exponential $SFR(t) \propto e^{-t/\tau}$
- Rising exponential (i.e. allow negative tau) $SFR(t) \propto e^{t/\tau}$
- Delayed exponential $SFR(t) \propto t\, e^{-t/\tau}$
- a la Sandage $SFR(t) \propto \frac{t}{\tau^2} e^{-\frac{t^2}{2\tau^2}}$

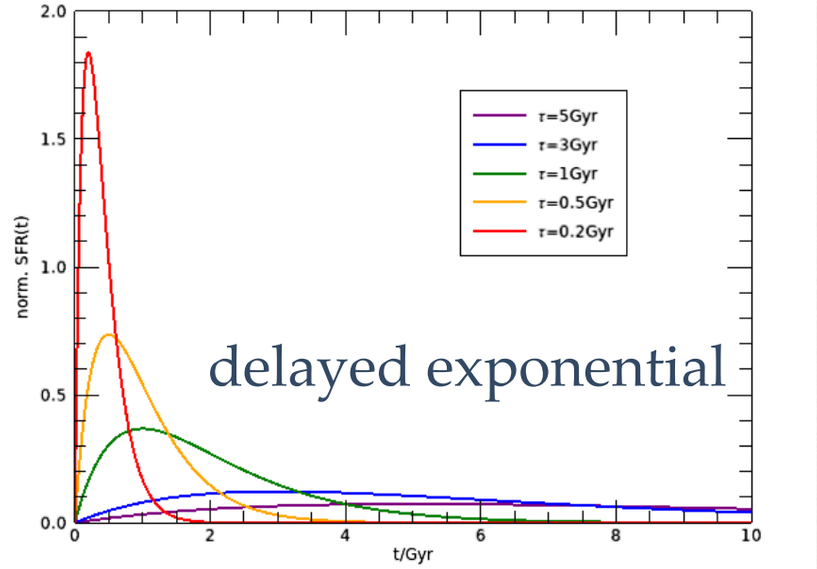

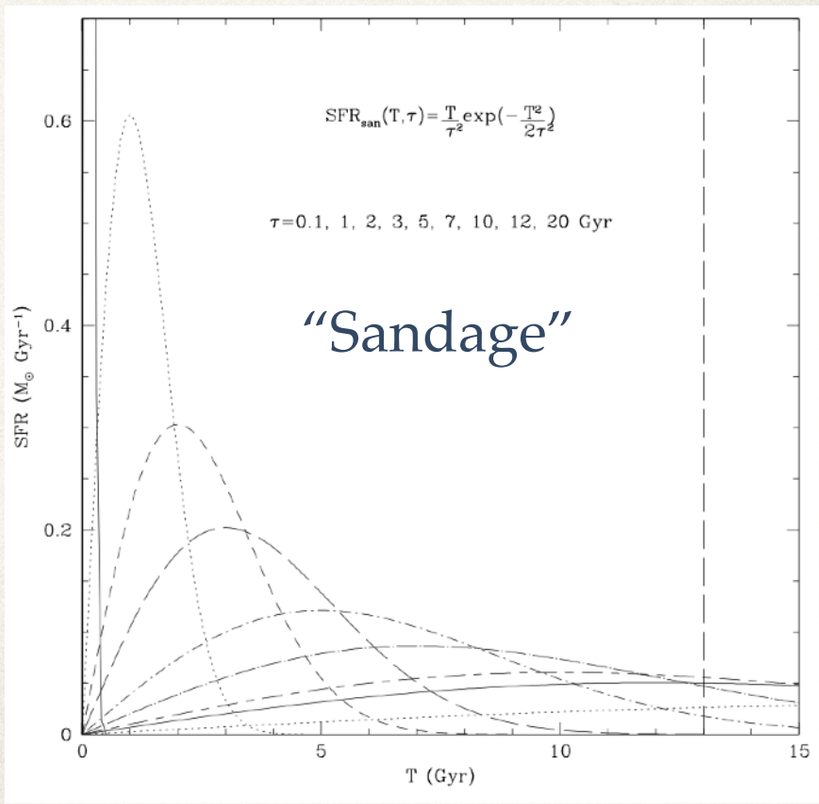

Examples of differences between SFHs

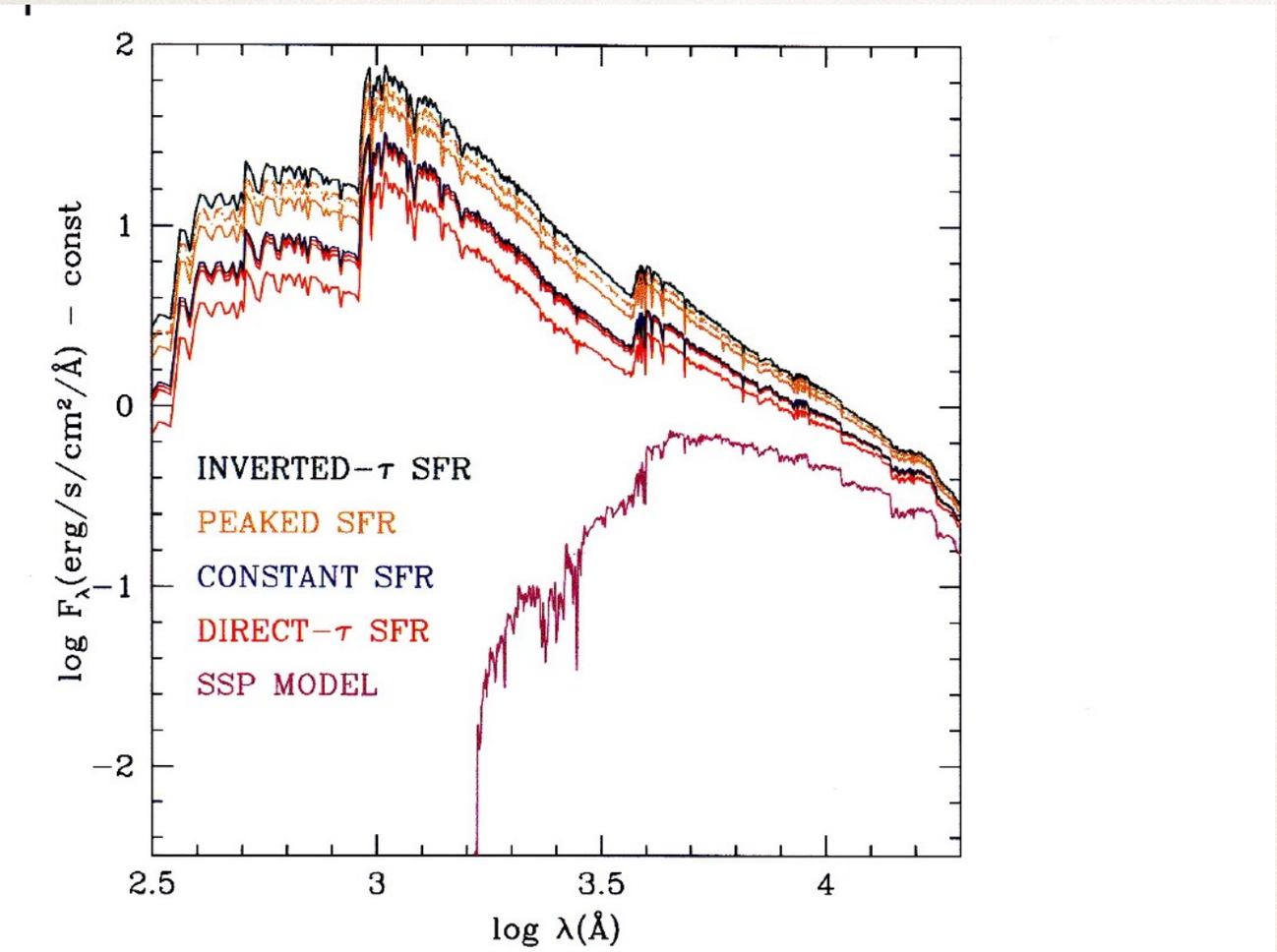

Figure C 5.4 Spectra of 1 Gyr old stellar populations with different past star-formation histories (SFH), but normalized to have formed the same mass of stars. Top to bottom the spectra refer to exponentially increasing SFRs with $\tau = 0.5$ Gyr, peaked SFH with $\tau = 1, 4, 7$ Gyr (the last two ones perfectly overlap), SFR = const., and exponentially decreasing SFR, with $\tau = 1, 4, 7$ Gyr (the latter two also overlap). For comparison the spectrum of a 1 Gyr old SSP is also shown (synthetic spectra kindly provided by C. Maraston).

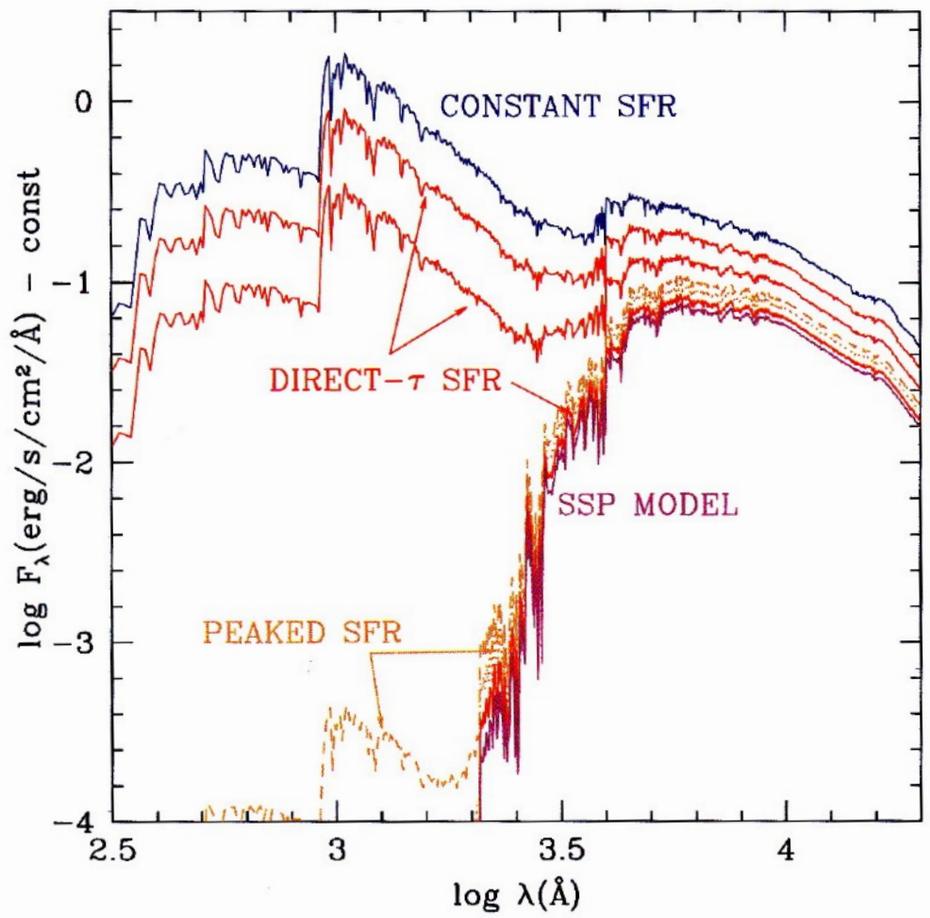

Figure C 5.5 The same as Figure 5.4 (without the inverted τ models) but for $t = 13$ Gyr. Displayed top to bottom are the spectra for a population with SFR = const., three spectra for direct-τ models with $\tau = 7$, 4, and 1 Gyr, then spectra for peaked SFHs with the same τ (largely overlapping). The spectrum of an SSP model for a 13 Gyr old population is also shown. Notice that the scale of the flux coordinate is consistent with that of Figure 5.4 (synthetic spectra kindly provided by C. Maraston).

Renzini & Greggio (2011), "Stellar populations"

Examples of differences between SFHs

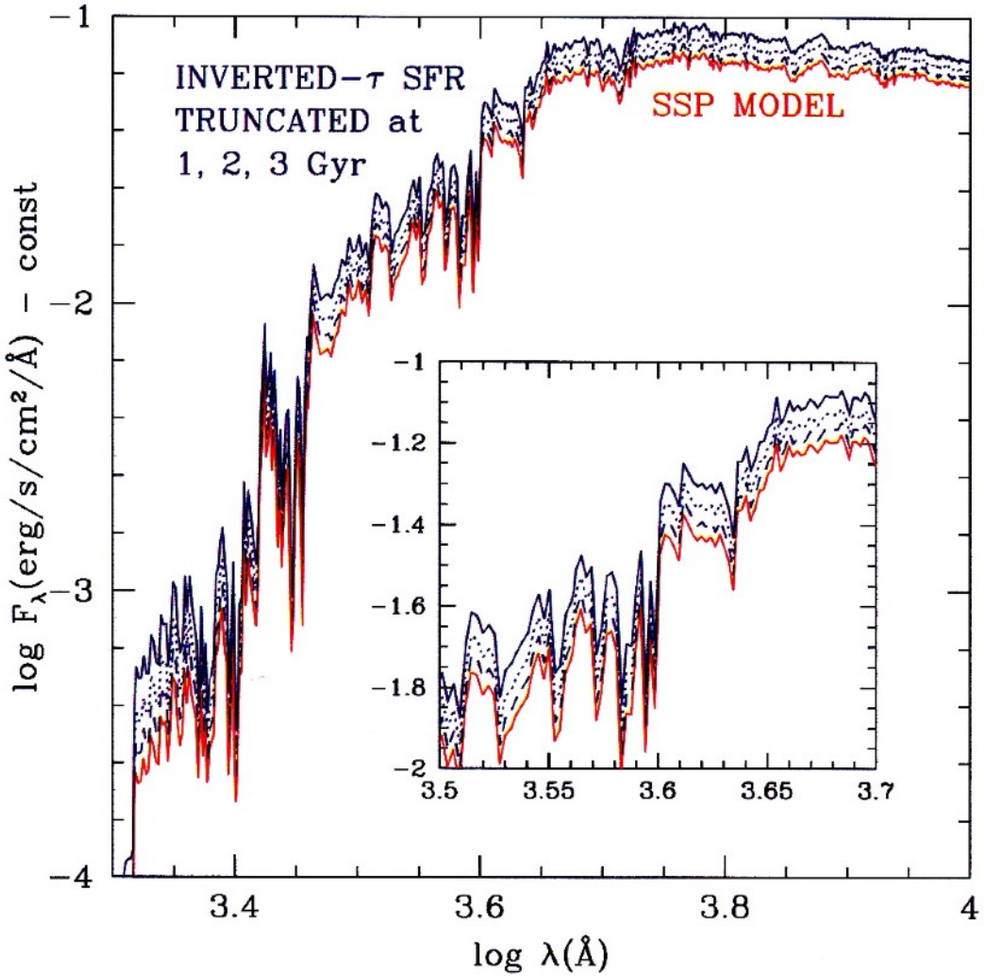

Figure C 5.6 The SSP spectrum at an age of 13 Gyr shown in Figure 5.5, now in an expanded scale, is compared to the spectra of $\tau = 0.5$ Gyr inverted-τ models with star formation truncated after 1, 2 and 3 Gyr. The insert shows a blow-up of the spectral regic around the Balmer/4000 Å break, to further illustrate the close similarity of all four spec tra (synthetic spectra kindly provided by C. Maraston).

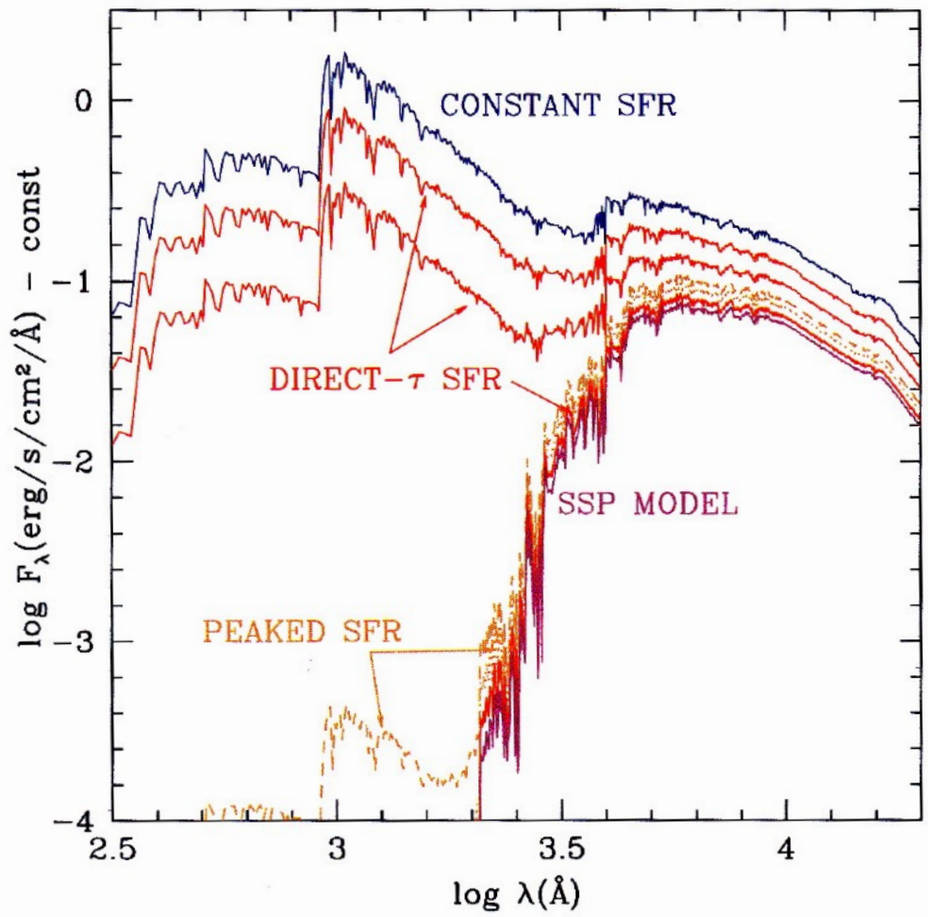

Figure C 5.5 The same as Figure 5.4 (without the inverted τ models) but for $t = 13$ Gyr. Displayed top to bottom are the spectra for a population with SFR = const., three spectra for direct-τ models with $\tau = 7$, 4, and 1 Gyr, then spectra for peaked SFHs with the same τ (largely overlapping). The spectrum of an SSP model for a 13 Gyr old population is also shown. Notice that the scale of the flux coordinate is consistent with that of Figure 5.4 (synthetic spectra kindly provided by C. Maraston).

Renzini & Greggio (2011), "Stellar populations"

Any hope to actually disentangle different SFHs???

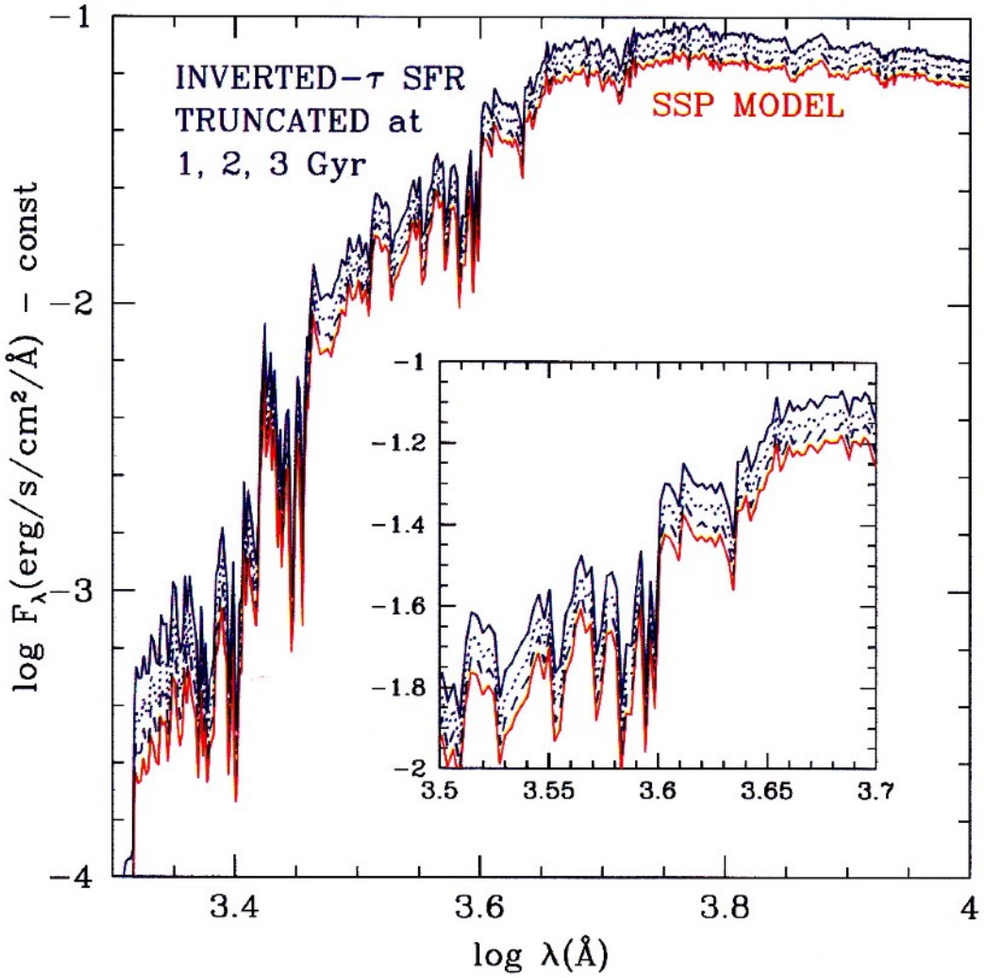

Figure C 5.6 The SSP spectrum at an age of 13 Gyr shown in Figure 5.5, now in an expanded scale, is compared to the spectra of $\tau = 0.5$ Gyr inverted-τ models with star formation truncated after 1, 2 and 3 Gyr. The insert shows a blow-up of the spectral regic around the Balmer/4000 Å break, to further illustrate the close similarity of all four spec tra (synthetic spectra kindly provided by C. Maraston).

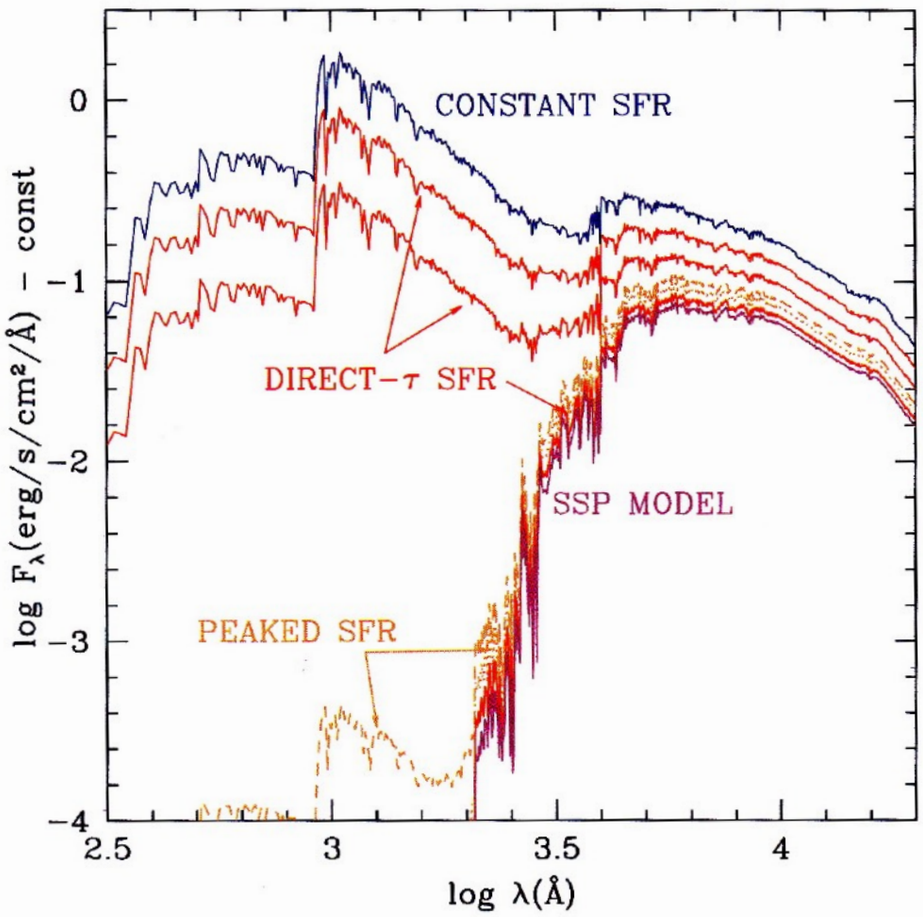

Figure C 5.5 The same as Figure 5.4 (without the inverted τ models) but for $t = 13$ Gyr. Displayed top to bottom are the spectra for a population with SFR = const., three spectra for direct-τ models with $\tau = 7$, 4, and 1 Gyr, then spectra for peaked SFHs with the same τ (largely overlapping). The spectrum of an SSP model for a 13 Gyr old population is also shown. Notice that the scale of the flux coordinate is consistent with that of Figure 5.4 (synthetic spectra kindly provided by C. Maraston).

Renzini & Greggio (2011), "Stellar populations"

Relative flux contribution of stellar evolutionary phases for prototypical galaxy SFHs

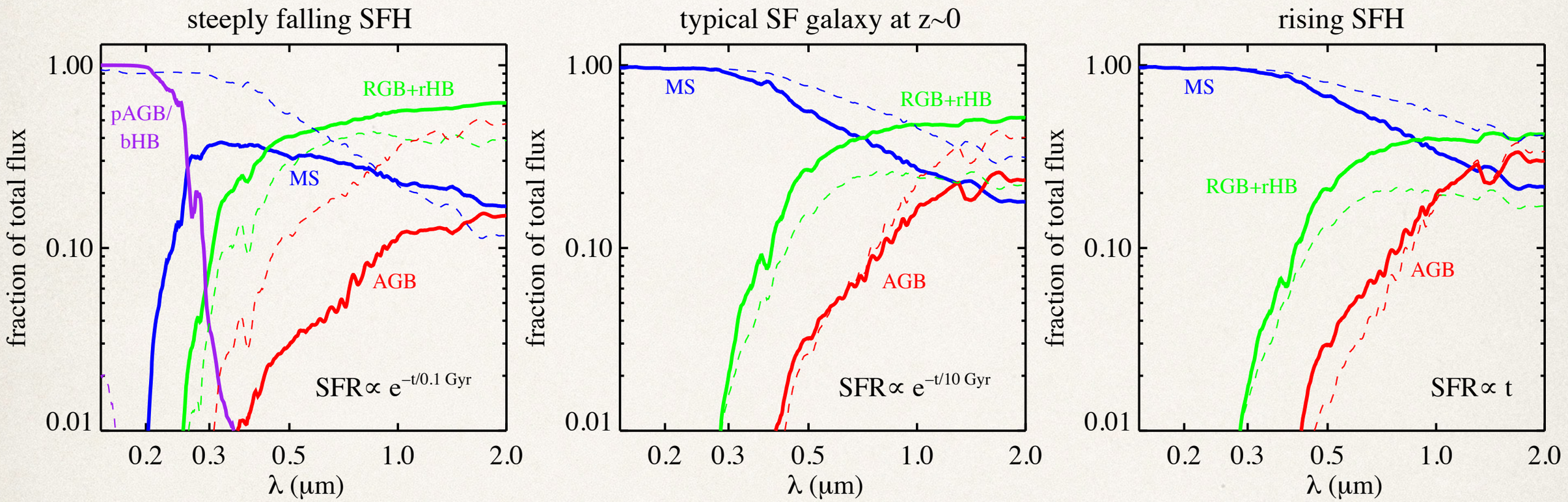

The left panel is representative of a galaxy that formed nearly all of its stars very rapidly at early times, the middle panel is representative of a typical star-forming galaxy at z ~ 0, and the right panel may be representative of the typical galaxy at high redshift. Flux contributions are at 13 Gyr (solid lines) and 1 Gyr (dashed lines) after the commencement of star formation; all models are solar metallicity, dust-free, and are from FSPS (v2.3; Conroy, Gunn & White 2009). Labeled phases include the main sequence (MS), red giant branch (RGB), asymptotic giant branch (AGB, including the TP-AGB), post-AGB (pAGB), and the blue and red horizontal branch (bHB and rHB).

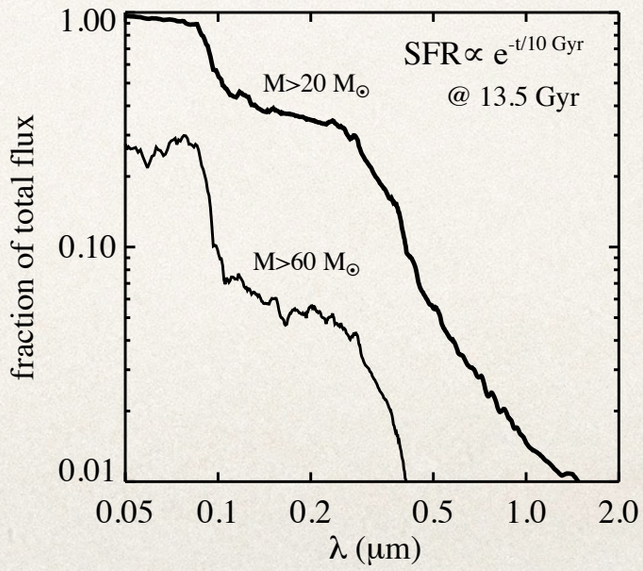

Conroy (2013)

Summary of Stellar Population Synthesis

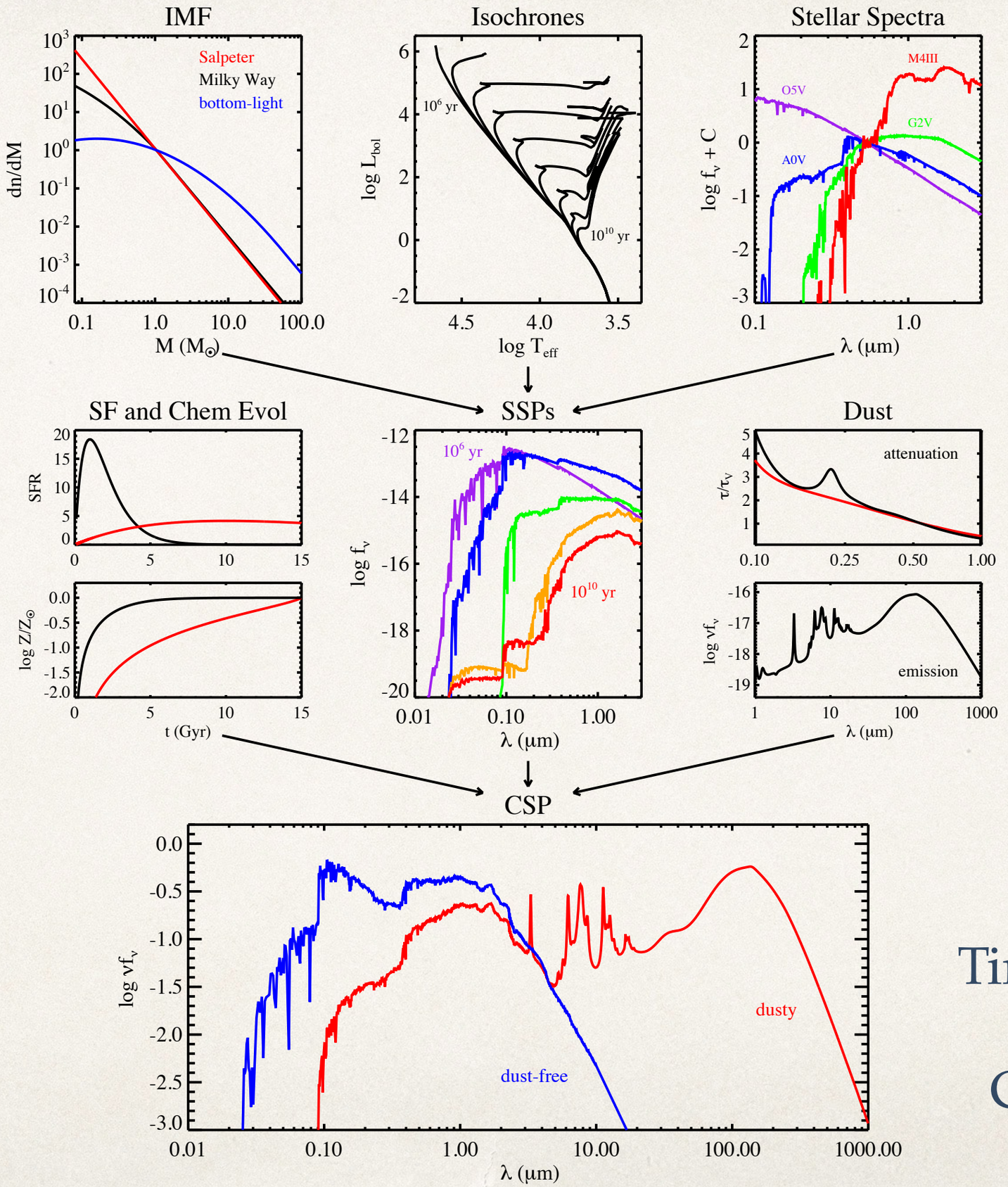

Tinsley (1972-80)

⇓

Conroy (2013)

Summary of Stellar Population Synthesis

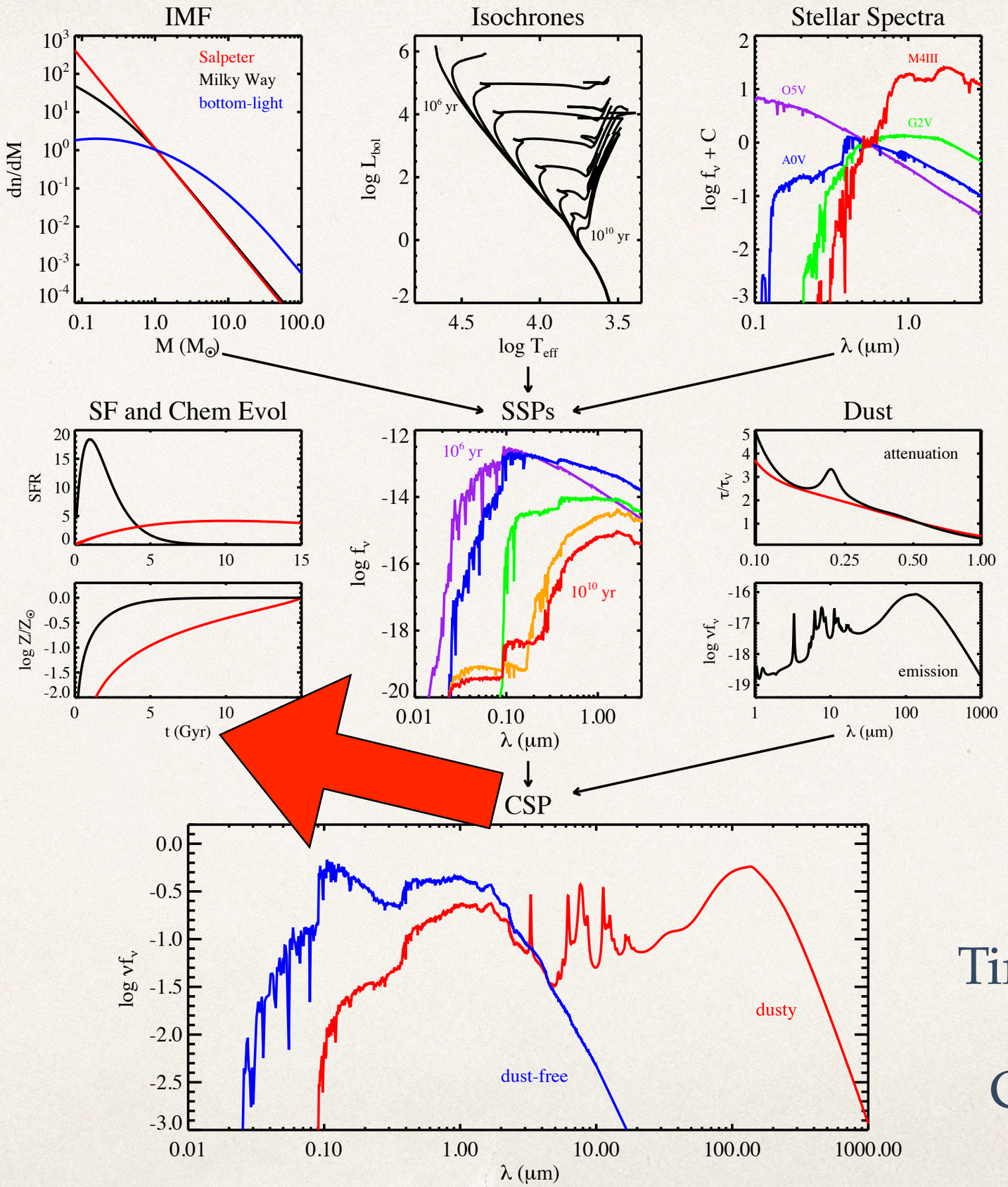

Tinsley (1972-80)

⇓

Conroy (2013)

The inversion problem

- Given a galaxy's SED (in a broad sense) we want to infer the stellar population parameters (and possibly dust attenuation as well)
  - stellar mass
  - mean stellar age
    - SFH
  - stellar metallicity
    - abundance distribution and patterns
- INVERSION of the physical assembly procedure described so far

The inversion problem: methods

- **Full inversion approach:** $F_{CSP} = \sum_i F_{SSP,i} \times w_i$, i running over ages, metallicities (dust, …)
  - retrieve SFH, Z distribution, dust as given by the weights $\{w_i\}$, via likelihood maximisation
  - non-parametric best fit, no explicit assumptions (which does not mean no bias!)
  - basically, the weight of each SSP is a free parameter to be fit (possibly a huge number!)
- **Bayesian inference**
  - (pre-computed) library of models
    - characterized by the observables to fit (colors, absorption features etc.)
    - labeled by physical parameters (M/L, <t>, <Z>, <[α/Fe]>...)
    - distributed according to a prior
  - comparison between real and model observables provides the likelihood (of the data given a model) to attach to each physical parameter
  - the probability distribution of the physical parameters is obtained via marginalization
- **PCA** (on models and data), machine learning methods etc.

The inversion problem: observables

- Broad/medium band SED: colors and shape of the SED

- Full spectrum

- Spectral features with high sensitivity towards age/metallicity/element abundances

- Observables must be optimized to the goals! i.e. they must be good tracers of the physical property one wants to retrieve

Stellar mass

- Extensive quantity, derived as M/L x L
  - M/L comes from models
  - L comes from observations
- Degenerate effect of 1) age, 2) metallicity and 3) attenuation on M/L AND optical colors: an increase of any of the three physical factors results in increasing M/L and make colors redder (e.g. Bell & deJong 2001)
- ⇒ optical colors and M/L tightly correlated

Bell & deJong (2001)

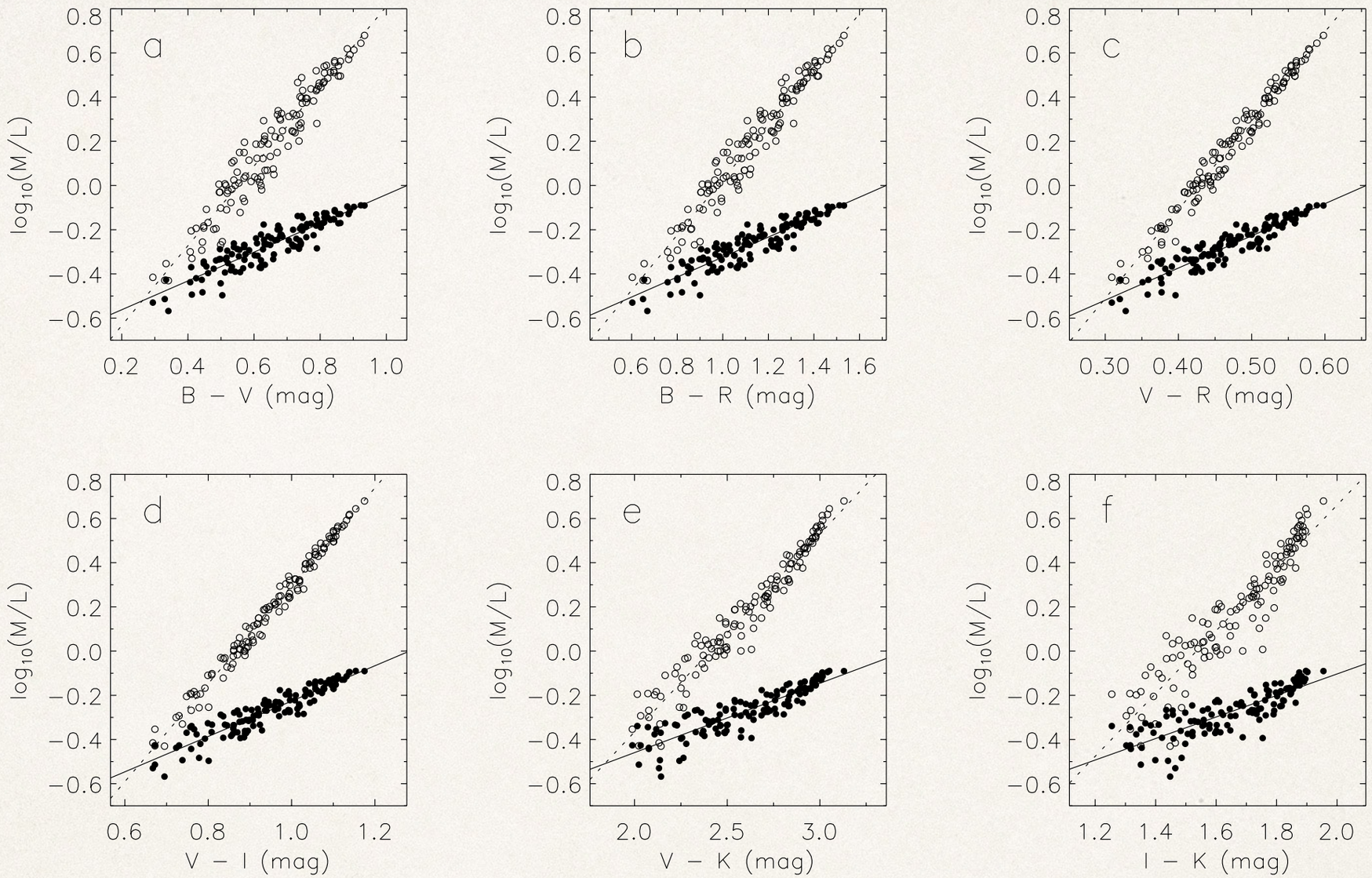

FIG. 9.—Trends in stellar M/L for the formation epoch model with bursts in K (*filled circles*) and B band (*open circles*) with (*a*) $B-V$, (*b*) $B-R$, (*c*) $V-R$, (*d*) $V-I$, (*e*) $V-K$, and (*f*) $I-K$ color. We also show the least-squares fit to the variations of stellar M/L ratio with color for the B-band (*dotted line*) and K-band (*solid line*) stellar M/L ratio.

scatter is not representative of real ***systematic*** uncertainties!

M/L beyond colors

- Observations of higher resolution SEDs (i.e. spectra!) and in particular age- and metallicity-sensitive features can help make a more precise characterization of the stellar population

- In general, precision does not increase dramatically wrt to colors only, due to the well known degeneracies. Improvement is significant for bursty SFH

- Absorption strengths are insensitive to dust (if all stellar populations see the same dust...) so one can infer only *intrinsic* M/L, whereas the *emerging* M/L (i.e. with L corrected for the attenuation) still require the use of the SED shape

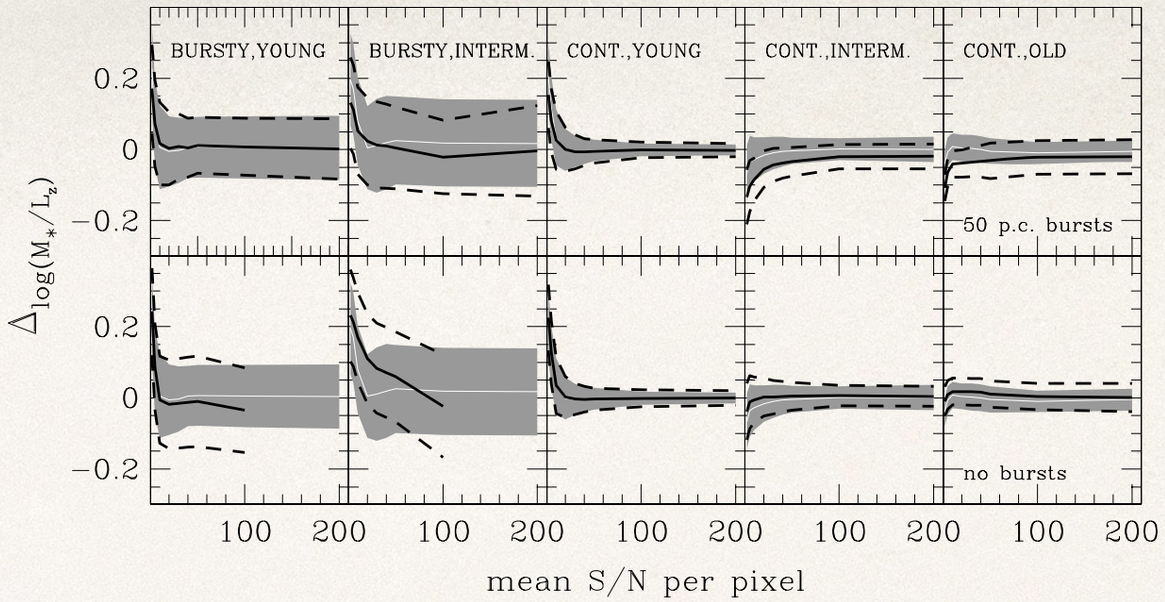

Figure 15. Offset between the retrieved and the true $\log(M_*/L_z)$ as a function of S/N for the five different spectral classes (as indicated in each panel). $\log(M_*/L_z)$ estimates are based on the spectral features $D4000_n$, the Balmer lines, $[MgFe]'$, and $[Mg_2Fe]$. The white line and the gray shaded region indicate the median and the rms, respectively, of $\Delta_{\log(M_*/L_z)}$ when the mock galaxies are fitted with the same model library from which they are drawn (as in Figure 4). In the bottom panels, the solid and dashed lines show the median and rms of the offsets for the case in which the mock galaxies are analyzed with a library without bursts. In the top panels, the black lines represent the results of fitting the mock galaxies with a burst-enhanced library.

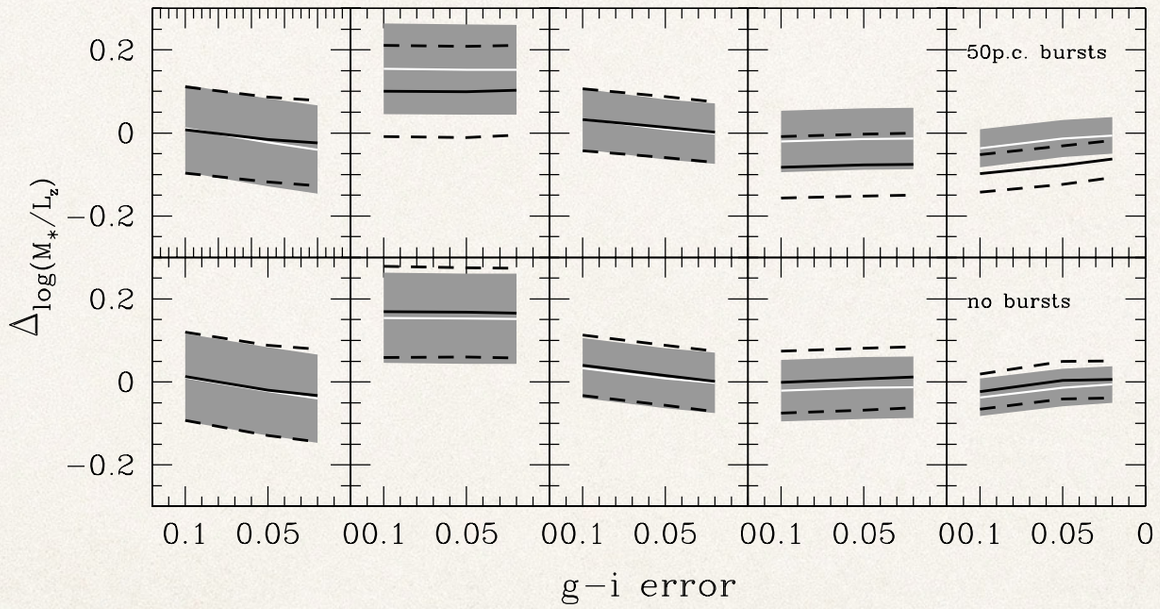

Figure 16. Offset between the $\log(M_*/L_z)$ estimated by fitting $g-i$ color and the true one as a function of the error on color (decreasing from left to right). The shaded region represents the distribution of offsets (median and rms) in the default case as shown in Figure 8. The solid and dashed lines show the median and rms of the offsets when the mock galaxies are analyzed with a library without bursts (bottom panels) or with higher probability of recent bursts (top panels).

Gallazzi & Bell (2009)

Stellar ages and metallicities

- ***Physically*** age and Z are coupled via the chemo-dynamical evolution of the galaxy, however this is hard to model
  - SSP equivalent
  - light-weighted or mass-weighted averages

$$\mathrm{Age}_{\mathrm{l.\text{-}w.}} = \frac{\int_{t=0}^{t_0} \mathrm{d}t\ (t_0 - t)\ \mathrm{SFR}(t)\ \mathscr{L}'(t)}{\int_{t=0}^{t_0} \mathrm{d}t\ \mathrm{SFR}(t)\ \mathscr{L}'(t)}$$

$$\mathrm{Age}_{\mathrm{M_*\text{-}w.}} = \frac{\int_{t=0}^{t_0} \mathrm{d}t\ (t_0 - t)\ \mathrm{SFR}(t)}{\int_{t=0}^{t_0} \mathrm{d}t\ \mathrm{SFR}(t)} = \frac{\int_{t=0}^{t_0} \mathrm{d}t\ (t_0 - t)\ \mathrm{SFR}(t)}{M_{*\,\mathrm{formed,tot}}}$$

  - full distribution (SFH and Z-distribution)

- ***Observationally*** age and Z are coupled via the well-known age-metallicity degeneracy (Worthey 1994, see next slides)

- ⇒ refined ***spectral*** diagnostics, high SNR observations

Age-Metallicity degeneracy

- *AGE* - Increasing age reddens the population by adding more luminosity to the RGB, removing hot stars from the MS.
- *METALLICITY* - Increasing Metallicity reddens the population by changing the high-temperature opacities.
  - Metallicity also reddens the population through increased line blanketing in cool phases.

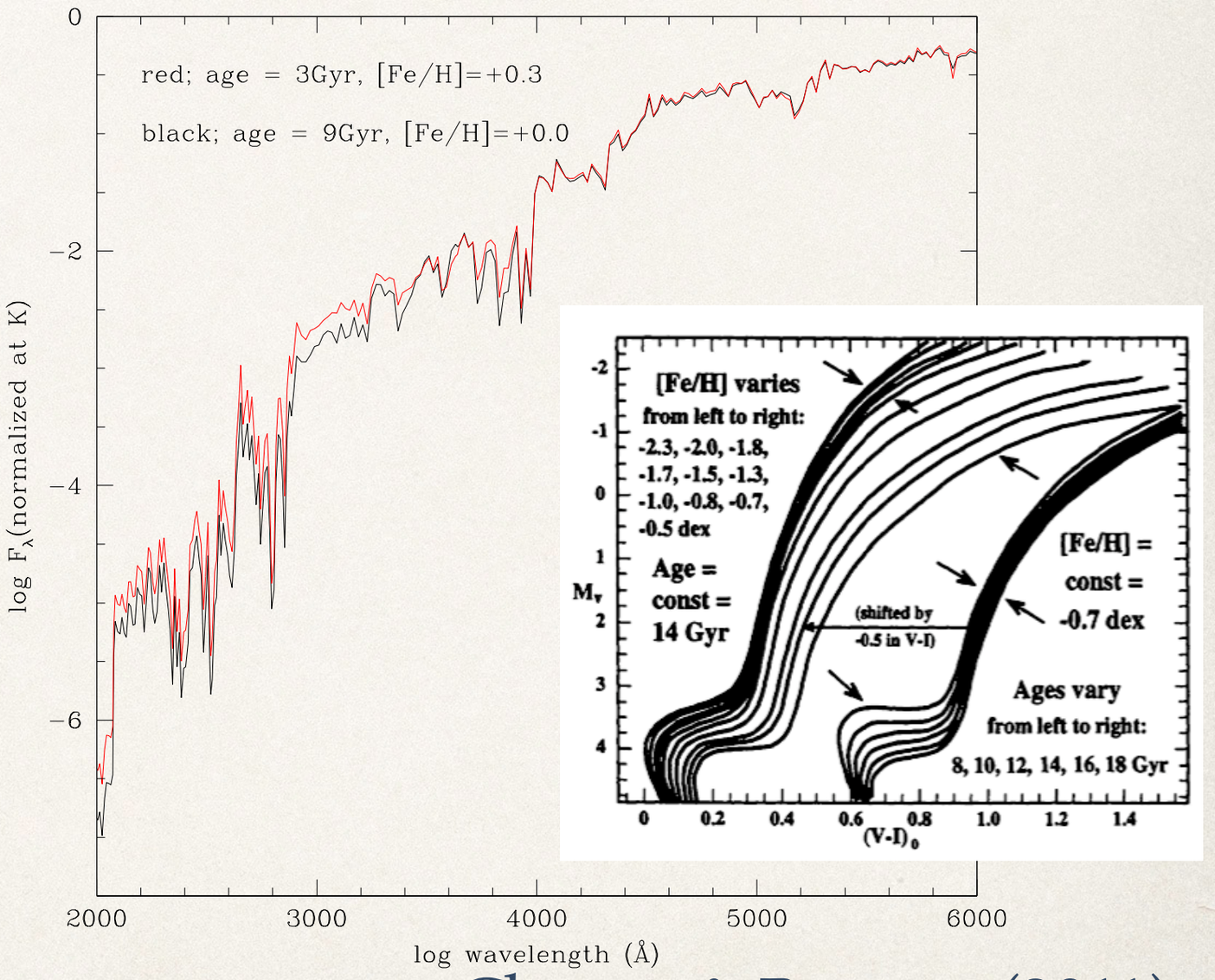

Chavez & Bertone (2011)

Colors only do not work...

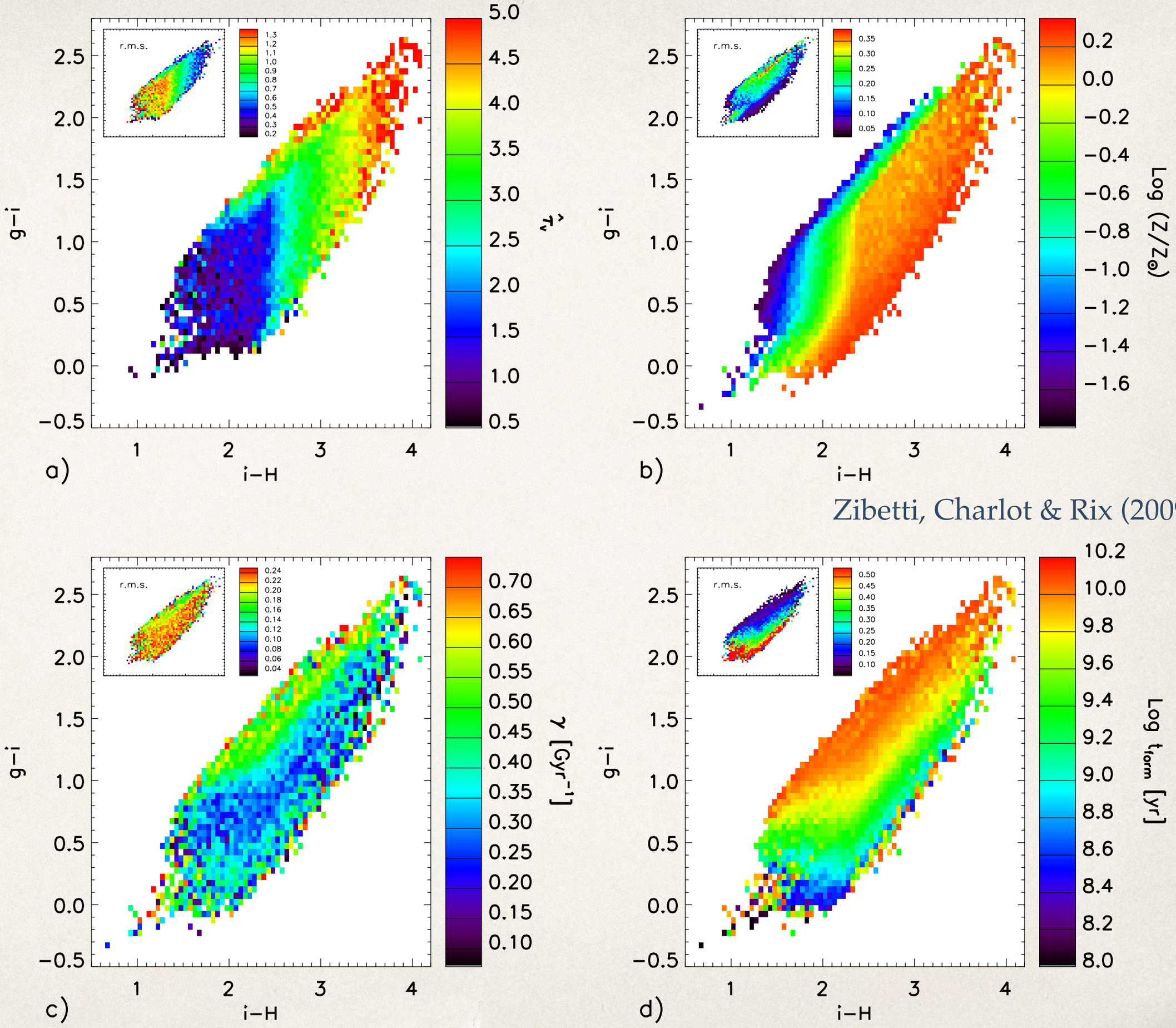

Zibetti, Charlot & Rix (2009)

Lifting the age-Z degeneracy

- As already proposed by Worthey (1994), spectral absorptions due to different elements (H, Fe, Mg, Ca etc) display different dependence on age and Z

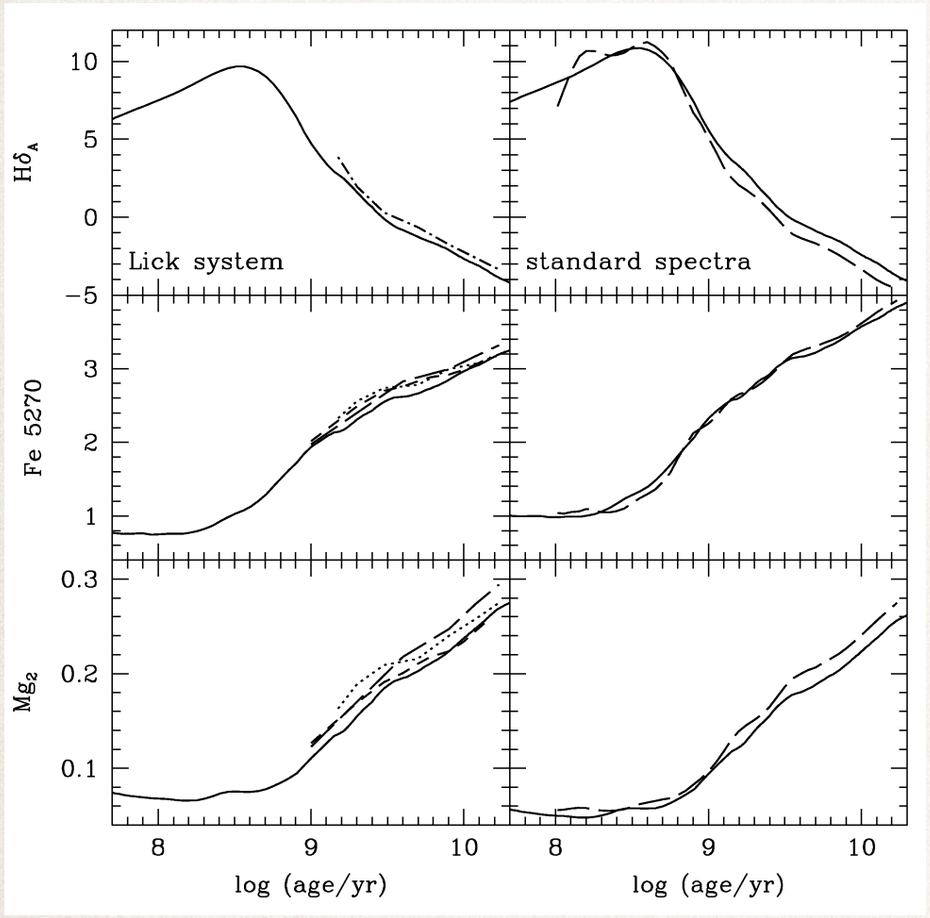

Bruzual & Charlot (2003)

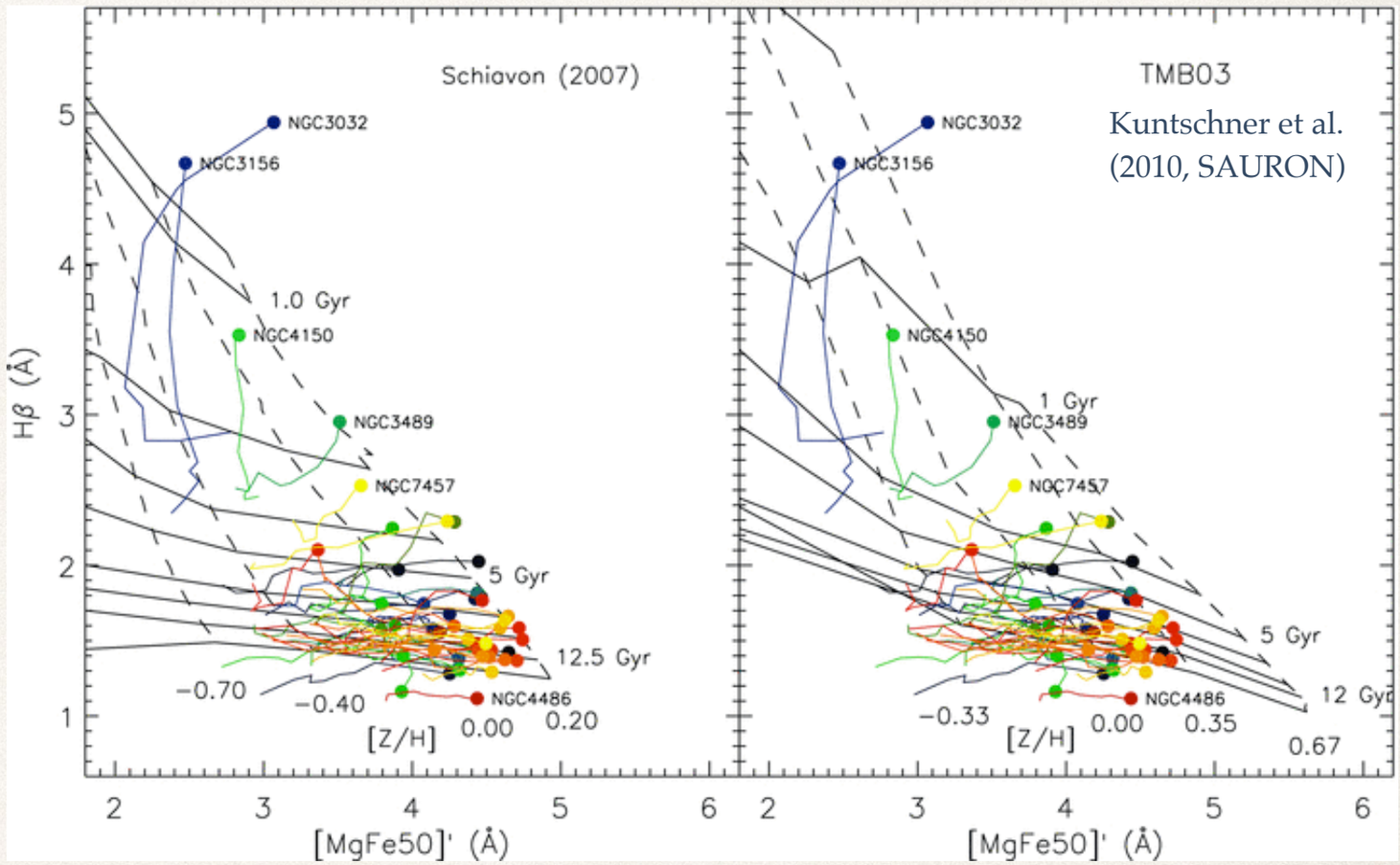

Grids of SSP models

⇓

"SSP equivalent" age/Z

Difficult to extend to complex SFH/ChEH and to multi-dimensional observational space

Lifting the age-Z degeneracy

- A set of few indexes with different sensitivity are sufficient to constrain average ages and metallicities to decent accuracy, provided that SNR in the spectra is good

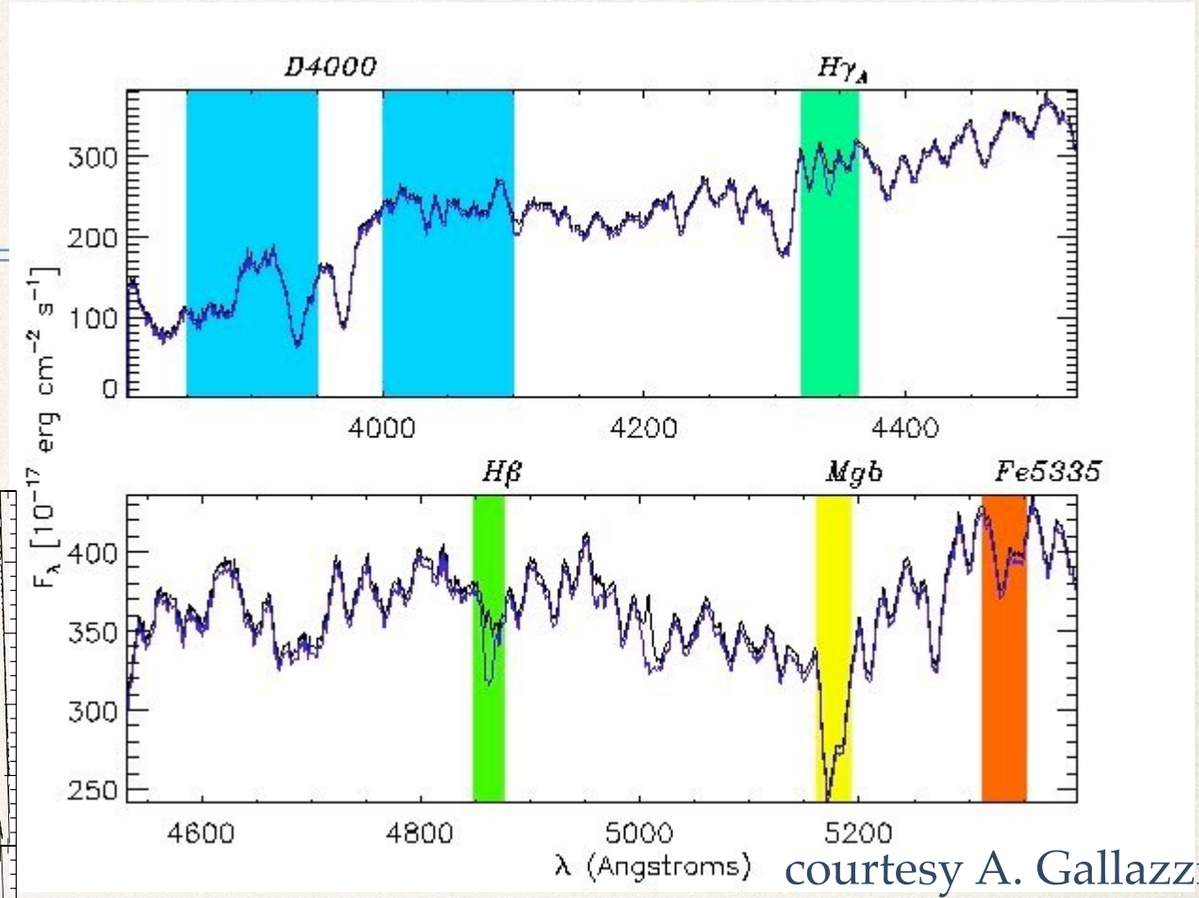

courtesy A. Gallazzi

- D4000, Hγδ and Hδ mainly sensitive to age, metal absorption to metals

Full set of indexes

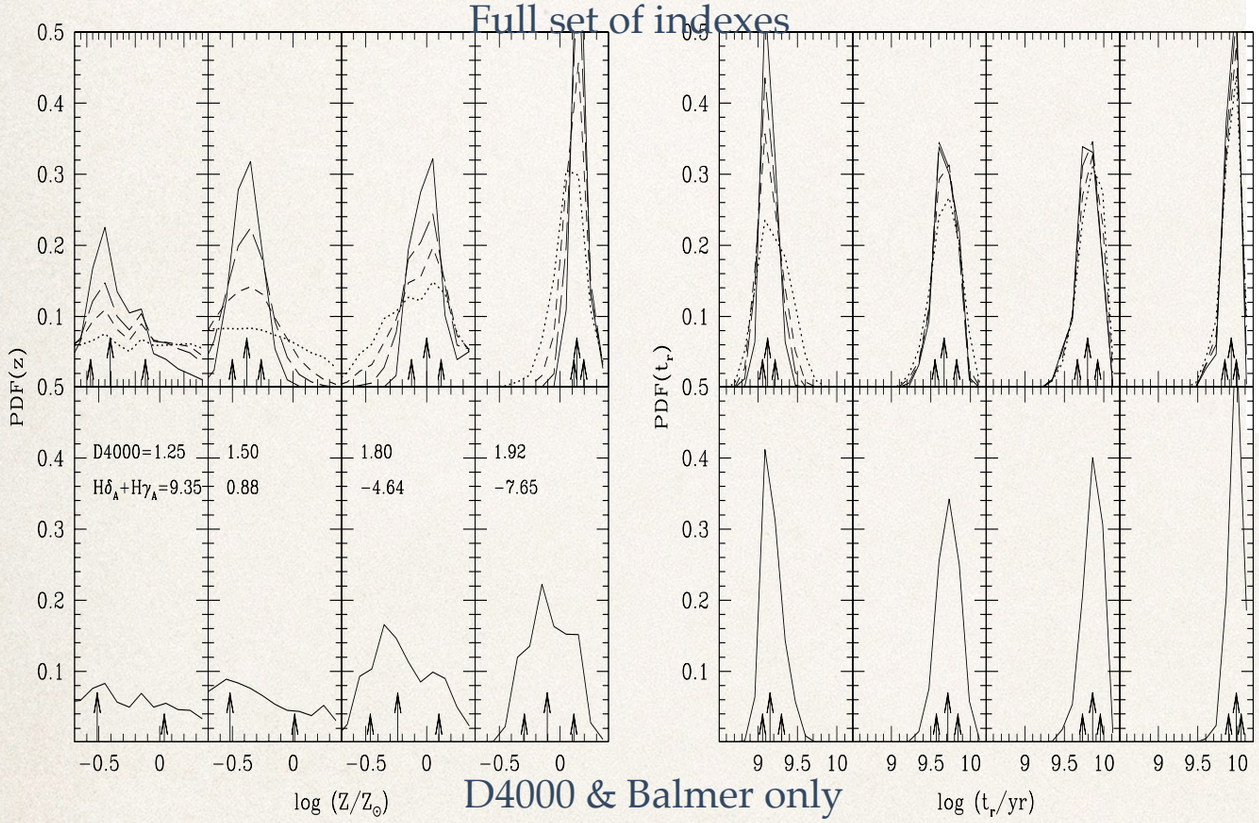

D4000 & Balmer only

Figure 3. Probability density functions of stellar metallicity (left-hand plot) and r-band light-weighted age (right-hand plot) for 4 SDSS galaxies with high-quality spectra (median S/N per pixel larger than 30) and different D4000 and $H\delta_A$+$H\gamma_A$ strengths (indicated in the bottom panels of the left-hand plot). The solid PDFs in the bottom panels were obtained when including only the age-sensitive indices D4000, $H\beta$ and $H\delta_A$+$H\gamma_A$ to constrain the fits. Those in the top panels were obtained after including also the metal-sensitive indices [Mg_2Fe] and [MgFe]′. In each panel, the arrows indicate the median (longer one) and the 16th and 84th percentiles (shorter ones) of the PDF. The long-dashed, short-dashed and dotted PDFs in the top panels show the constraints obtained when degrading the original galaxy spectra to a median S/N per pixel of 30, 20 and 10, respectively (see text for detail).

Gallazzi et al. (2005)

Theoretical dependence of parameters on indices

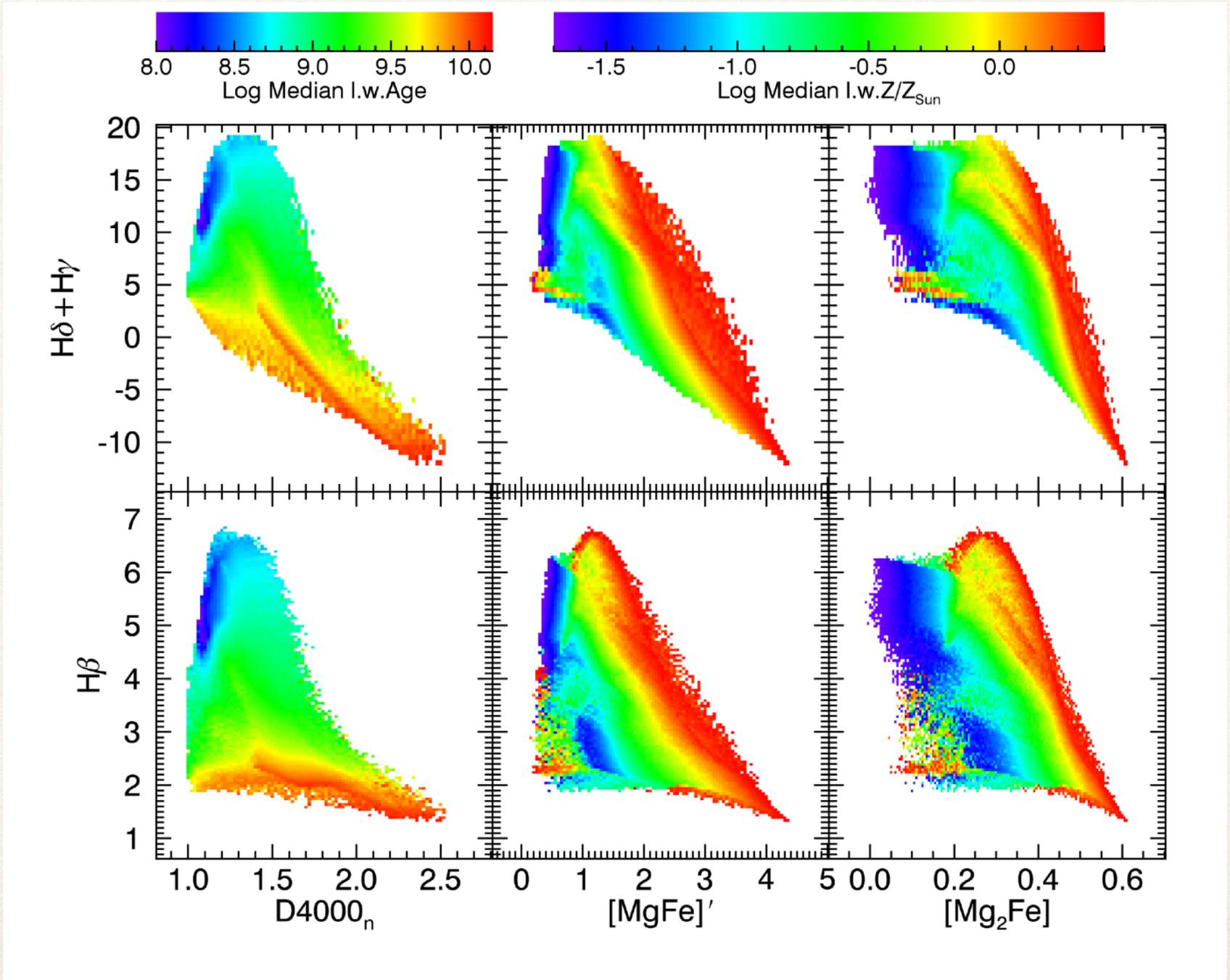

Method: bayesian likelihood marginalisation

- Precomputed library of models with attached physical parameters (the unknowns in real galaxies) and synthetic observables
  - The density distribution of models in the space of physical parameters gives the **prior probability distribution**
- For each model we define the **likelihood function** (="probability of the data given a model") via comparison between its synthetic observable and real data observables (typically $P \propto \exp(-\chi^2)$)
- The **posterior probability distribution** (="probability of a model parameter given the data") is then proportional to "prior probability distribution" times the "likelihood function"
- Not all parameters are of interest (certainly not all simultaneously!) so one has to collapse the multi-dimensional space of physical parameters and retain only the interesting dimension(s), i.e. one has to **marginalise**
- Analyse the marginalised posterior probability **function**!
  - Quantiles provide **uncertainties**
- *Goal*: make likelihood dominate over prior, i.e. let data decide - high quality dataset and optimal diagnostics
- **Advantages** over best fit approach:
  - robust against **degeneracies**!
  - the PDF naturally provides estimate uncertainties, hard to get in the frequentist approach

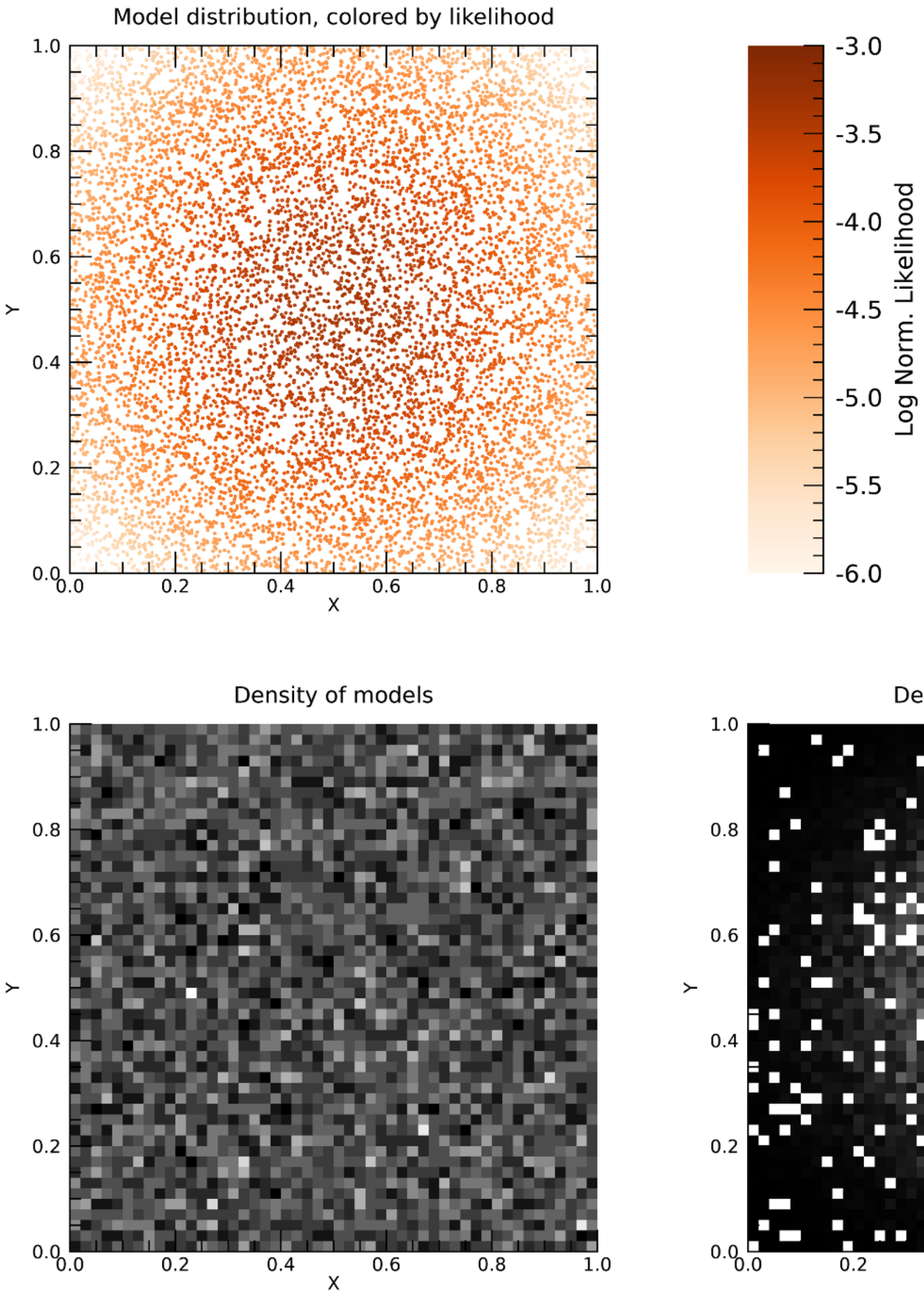

Bayesian statistics at work

Age-Z, the bayesian estimates

Bivariate age-Z probability distribution function (PDF)

$$P(\langle t\rangle,\langle Z\rangle) \propto P(\text{data} \mid \text{models}(\langle t\rangle,\langle Z\rangle)) * P(\text{models}(\langle t\rangle,\langle Z\rangle))$$

- SFH:
  - exponentially decaying, two parameters t_0 and timescale
  - random bursts
  - delayed SFH more popular esp. for high z (e.g. Maraston+11)
- Z-distribution
  - flat in linear or log
- dust, can be included or estimated a posteriori, but requires colors!

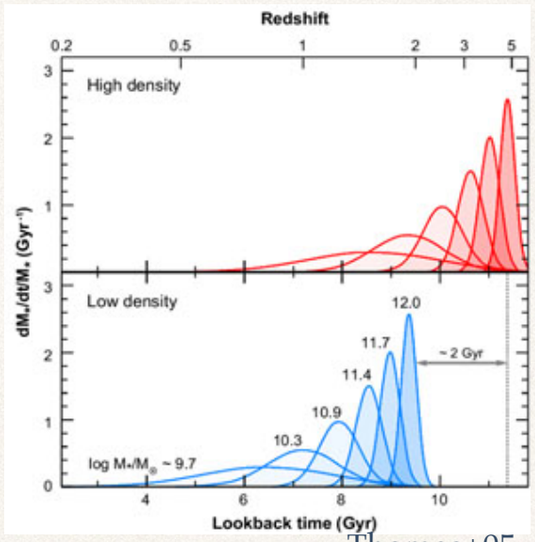

Thomas+05

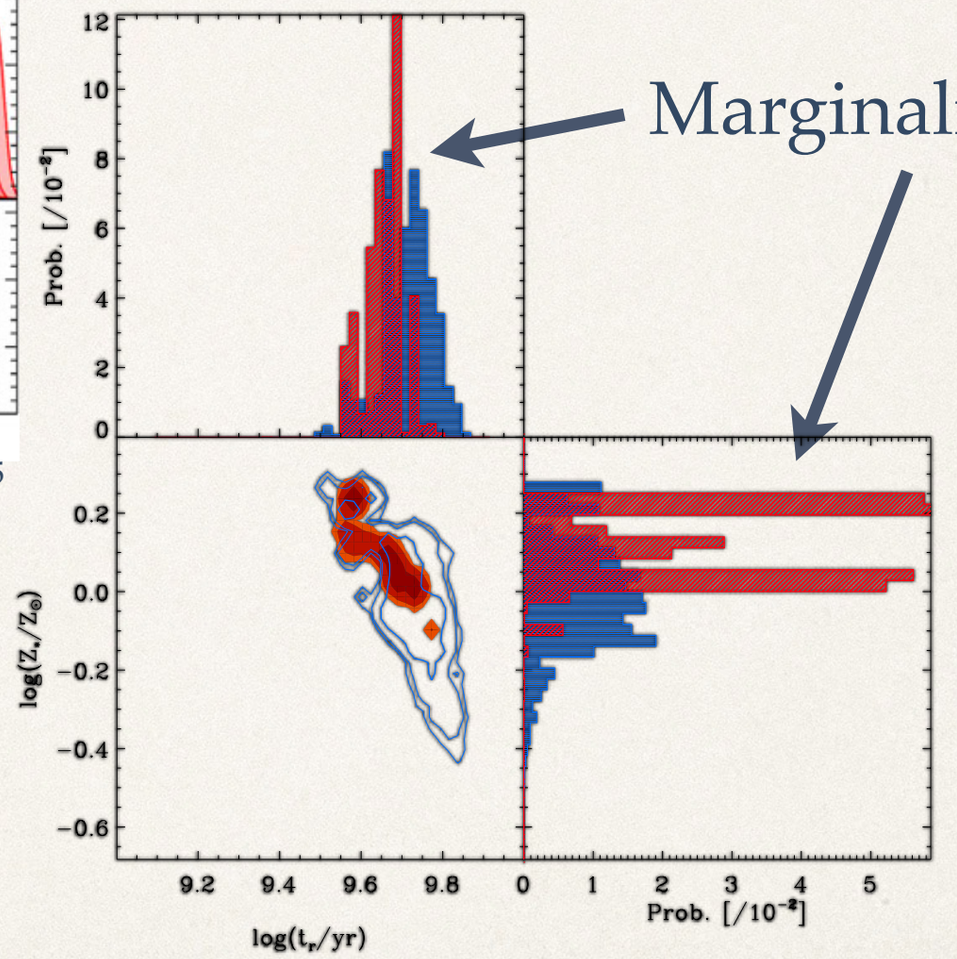

Marginalization

Red-blue: two different priors

courtesy A. Gallazzi

Application to large spectra datasets (SDSS)

44,254 SDSS-DR2 galaxies with median S/N per pixel >20 (Gallazzi et al. 2005)

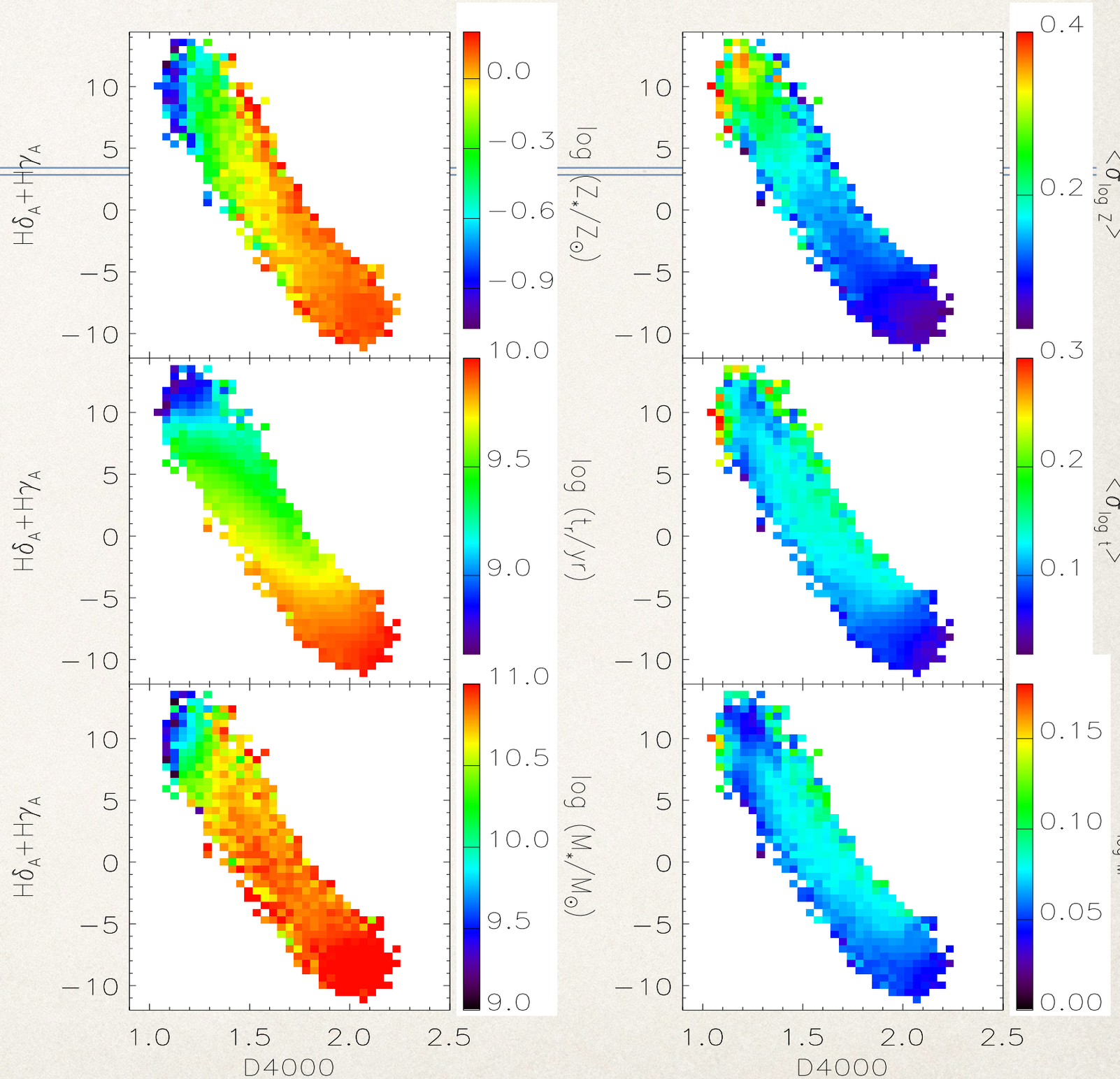

SFH indicators: continuous vs bursty

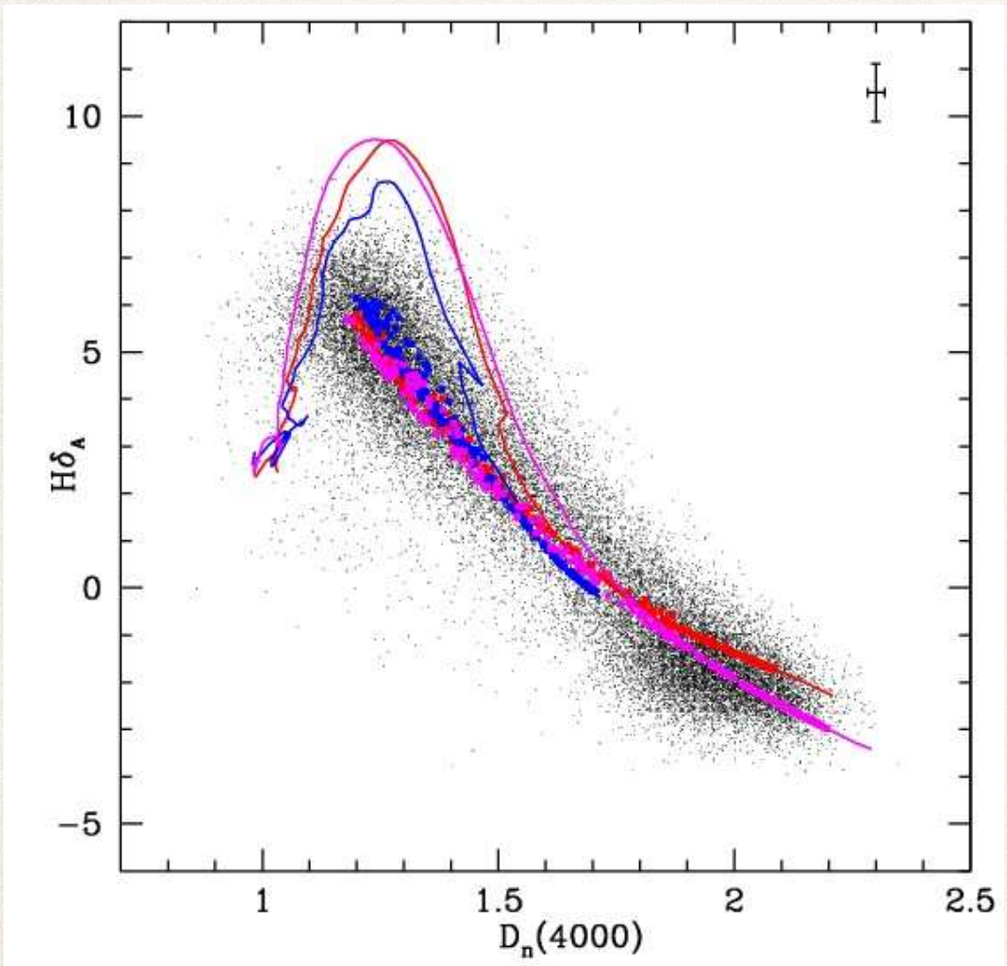

Figure 3: $H\delta_A$ is plotted as a function of $D_n(4000)$ for 20% solar, solar and 2.5 times solar metallicity bursts (blue, red and magenta lines), and for 20% solar, solar and 2.5 solar continuous star formation histories (blue, red and magenta symbols). A subset of the SDSS data points with small errors are plotted as black dots. The typical error bar on the observed indices is shown in the top right-hand corner of the plot.

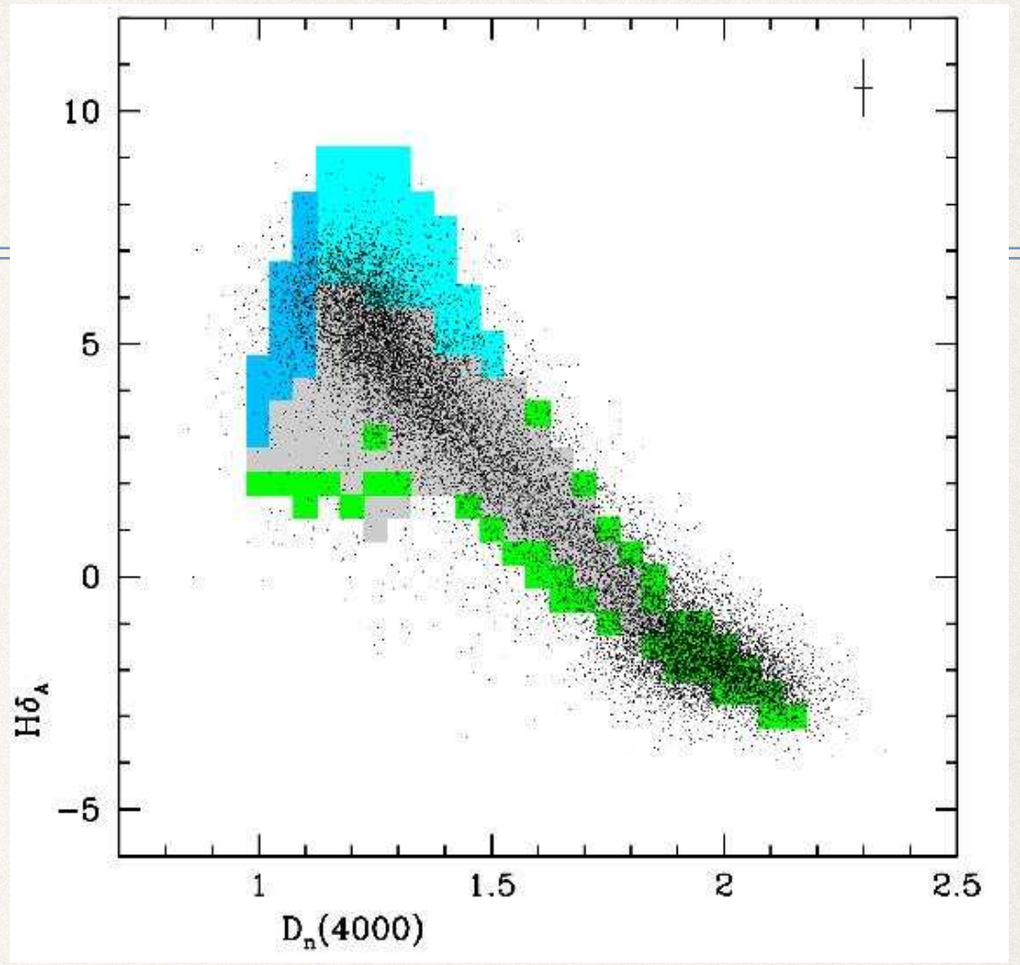

Figure 6: The $D_n(4000)/H\delta_A$ plane has been binned and colour-coded to reflect the fraction of simulated galaxies with F_{burst} in a given range. Blue indicates regions where 95% of the model galaxies have $F_{burst} > 0.05$ and the onset of the burst occurred more than 0.1 Gyr ago. Cyan indicates regions where 95% of the model galaxies have $F_{burst} > 0.05$ and the onset of the burst occurred less than 0.1 Gyr ago. Green indicates regions where 95% of the model galaxies have $F_{burst} = 0$. Grey indicates all other regions covered by the model galaxies.

Kauffmann et al. (2003)

Dust attenuation

- Affects the colors (i.e. the overall shape/slope of the SED) but very little the indices (D4000 is the most affected, being de facto a color)

- Index analysis can be performed using libraries with or without dust as well

  - The strength of attenuation can be derived a posteriori for each model by comparing colors

  - Dust attenuation can be already hard-coded in models (e.g. with the 2-component prescription of Charlot & Fall 2000, or Chevallard et al. 2013). In this case colors must be taken into account in the fitting procedure (eg concur to the likelihood of the model)

"α enhancement"

- Ratio of α-elements (O, Ne, Mg, Si, S, Ar, Ca, Ti) to iron-peak elements (Fe, V, Cr, Mn, Co and Ni) provides important information about the prevalent type of SN that enriched the protostellar gas
  - α-elements are enhanced in core collapse SN: massive, short lived stars, time scale of few 10^8 yr
  - Fe-peak mainly from SN Ia: evolved binary system, time scale $\gtrsim 10^9$ yr
- Information about the chemical enrichment (and SFH) time scale
- Most models are tuned to solar abundance patterns, but new coming online (Walcher, Coelho +2009): direct comparison with data not trivial
- Empirical estimates to derive qualitative trends (e.g. showing that more massive ellipticals had shorter timescales wrt less massive ones, Thomas+05)

SFH reconstruction

- Pros: more degrees of freedom
  - no bias from pre-defined SFH
  - independent Z and dust attenuation for different components
- Cons: amount of information cannot be expanded ad libitum
  - need to reduce the time bins or
  - have to deal with biases and ill-behaved solutions (e.g. tendency to pick up preferential time solutions corresponding to the epoch of main stellar pop transitions: OB-AF-G-KM stars!)
  - regularizations can be applied (but this is like introducing info by hand)
  - Need very high SNR in order to obtain more than 3-4 bins

SFH reconstruction via inversion

- MOPED (Heavens, Jimenez, and Lahav 2000)
- VESPA (Tojeiro et al. 2007)
- STECKMAP (Ocvirk et al. 2006)
- STARLIGHT (Cid Fernandes et al. 2005)
- sedfit (Walcher et al. 2006), Paradise (Walcher et al. 2009)
- NBURSTS (Chilingarian et al. 2007)
- ULySS (Kolevaet al. 2009).

Example: VESPA (Tojeiro+07)

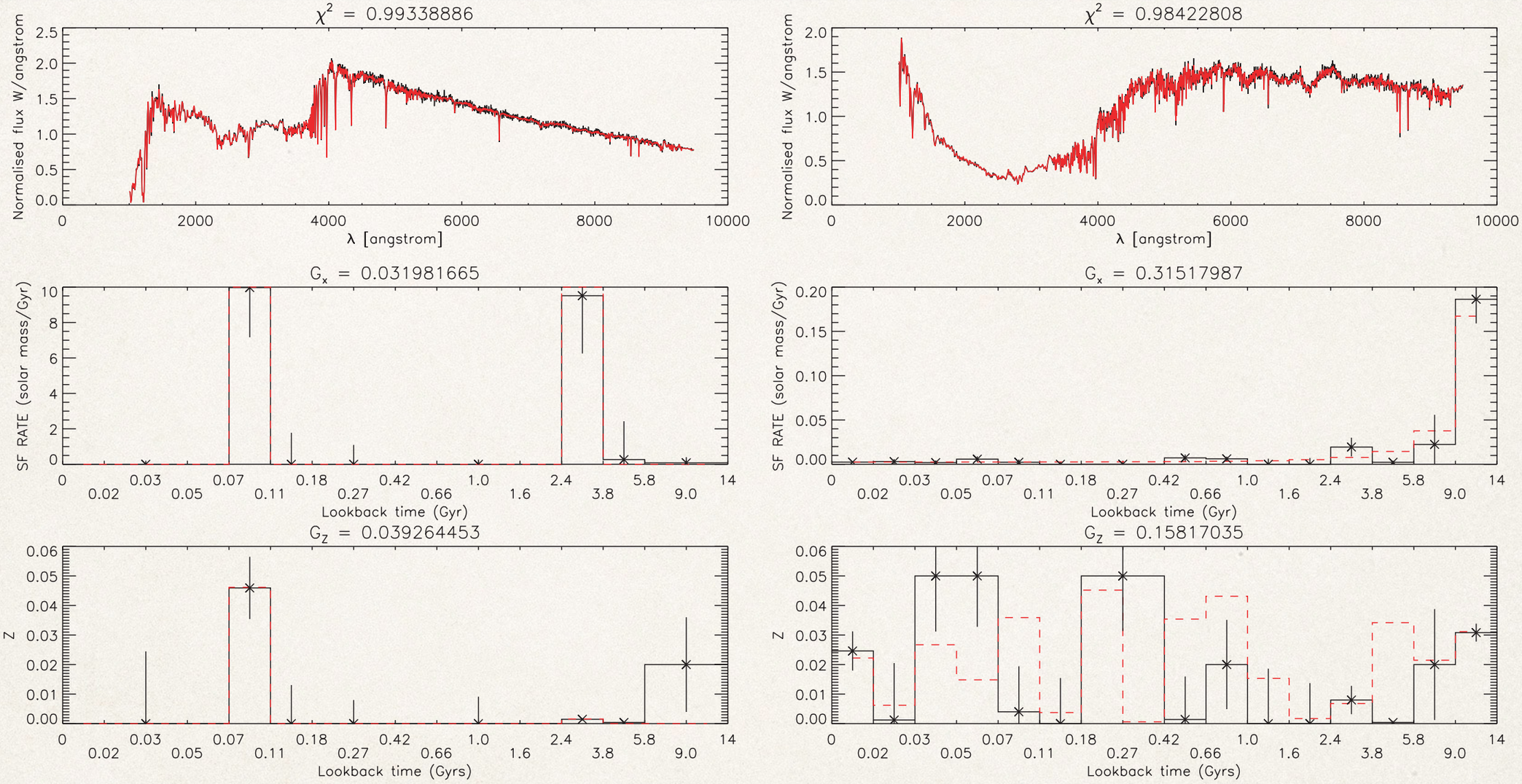

Figure 4. Two examples of VESPA's analysis on synthetic galaxies. The top panels show the original spectrum in the dark line (black in the online version) and fitted spectrum in the lighter line (red in the online version). The middle panels show the input (dashed, red) and the recovered (solid, black) SFRs and the bottom panel shows the input (dashed, red) and recovered (solid, black) metallicities per bin. Note that even though many of the recovered metallicities are wrong, these tend to correspond to bins with very little star formation, and are therefore virtually unconstrained.

Example: VESPA (Tojeiro+07)

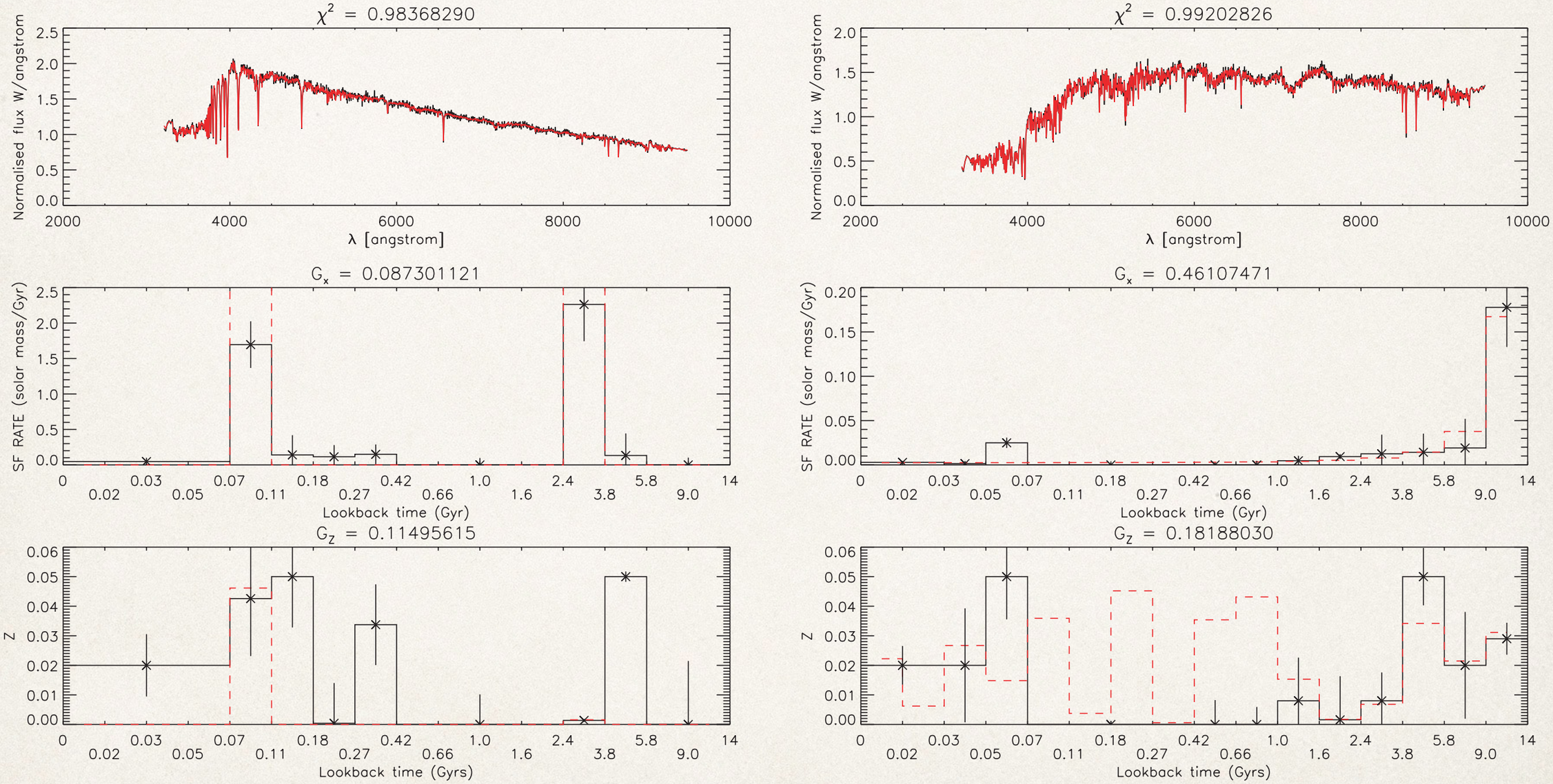

Figure 6. Same galaxies as in Fig. 4, but results are obtained by using a smaller wavelength range. The goodness of fit in data space is still excellent, but it becomes more difficult to break certain degeneracies.

Example: STARLIGHT (Cid Fernandes +05)

No assumptions on SFH does not mean no bias...

Look at the peaks!

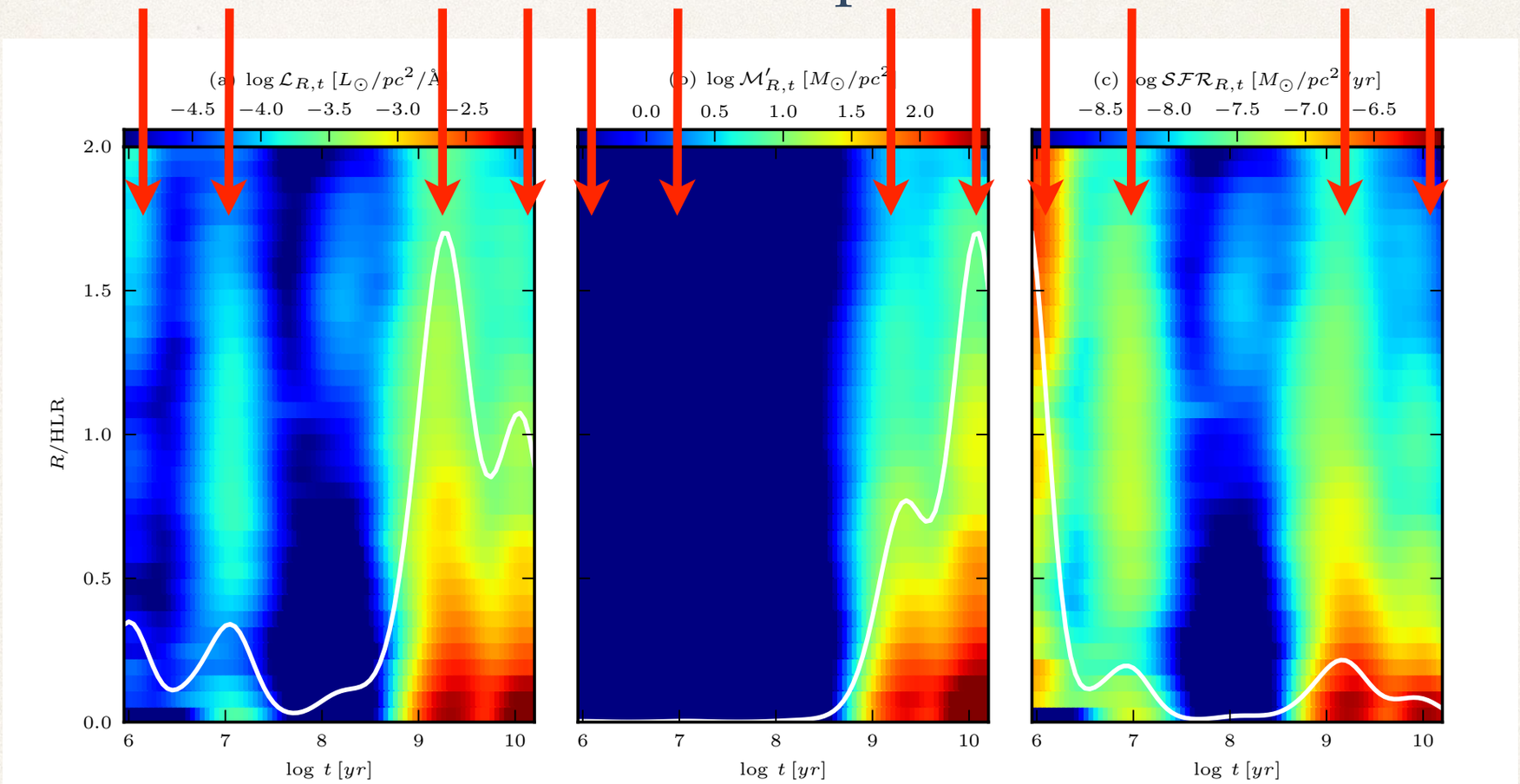

Fig. 12. *R-t* diagrams showing the radially averaged distribution of light, mass and SFR as a function distance from the nucleus and age. *Left:* Luminosity at λ = 5635 Å per unit area. ($\mathcal{L}_{R,t}$). *Middle:* Stellar mass formed per unit area ($\mathcal{M}'_{R,t}$). *Right:* Time dependent SFR per unit area ($\mathcal{SFR}$). The solid (white) lines represent the sum over all spaxels for a given age.

Cid Fernades +13

Need for “regularization”

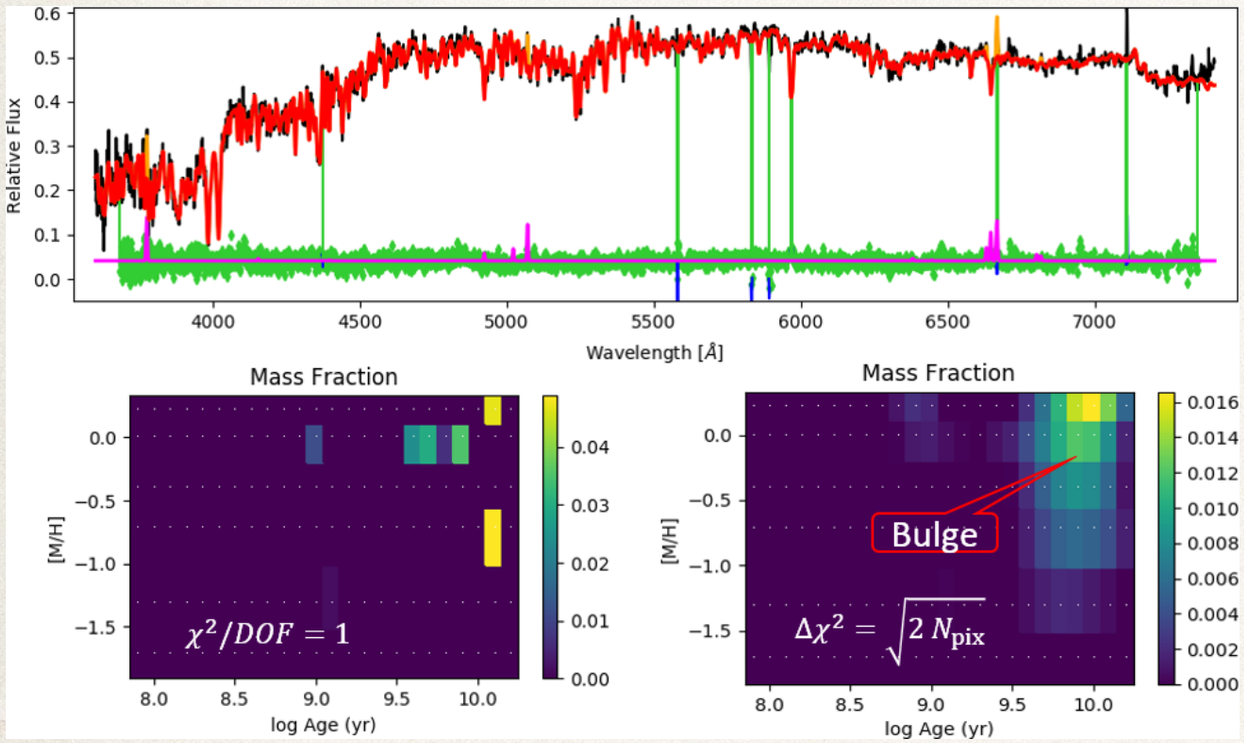

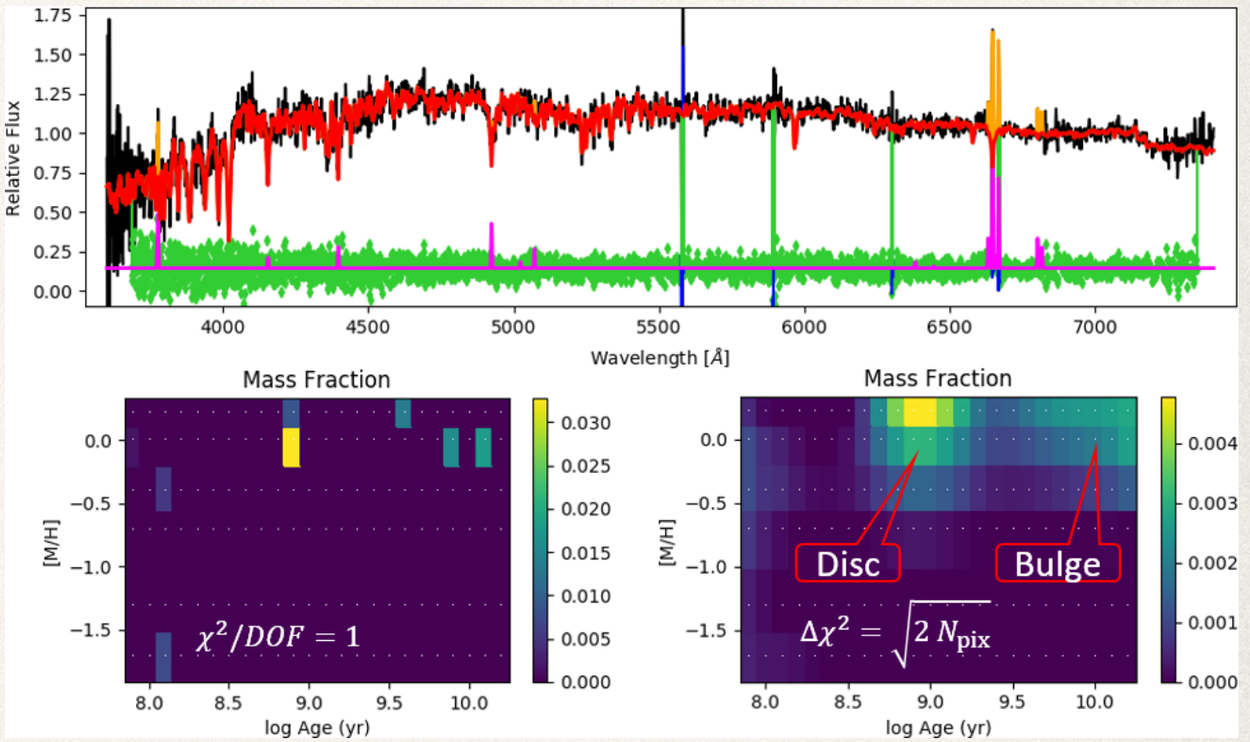

From Michele Cappelari’s webpage

Figure 3: Population and gas with pPXF. *The plots show the pPXF fit to two MaNGA spectra for the spiral galaxy NGC2916 (from SDSS DR13). The* ***Left Spectrum*** *is located in the galaxy bulge, while the* ***Right Spectrum*** *is in the disk. The "Mass Fraction" maps, below each spectrum, show the corresponding pPXF solution in different age and metallicity intervals. The* ***Left Maps*** *have no regularization. These are the minimum χ^2 solutions which all non-regularized full-spectrum fitting programs must return, if they properly converge. However these solutions are noisy and arbitrary as this inverse problem is ill-posed. Regularization is a standard approach to solve ill-posed problems (see Cappellari 2017, Sec.3.5). The* ***Right Maps*** *show the pPXF regularized solutions: here one can clearly recognize the change in the relative contribution of bulge (~10Gyr) and disk (~1Gyr) stars at the two spatial locations. The fits used as templates a subset of 24(Ages)×6([M/H])=144 MILES model spectra by Vazdekis et al. (2010), and 12 gas emission lines.*

Indices vs full spectrum fitting

Indices

- Well tested response on change of stellar parameters
- Require high SNR and waste a lot of valuable info
- Insensitive to dust, require separate/additional fitting of colors
- Insensitive to spectral flux calibration
- Insensitive to unknown bugs in models (fake features!)

Full spectrum

- Redundant information help beating SNR issues, incomplete coverage (e.g. in regions contaminated by nebular emission)
- simultaneous contribution of high and low frequencies (good or bad??)
- dust sensitive
- flux calibration issues
- model bug sensitive...

Stellar Initial Mass Function

- Salpeter '55
- Miller & Scalo '79
- Kennicutt '83
- Scalo '86
- Kroupa, Tout & Gilmore '93
- **Kroupa '01**
- **Baldry & Glazebrook '03**
- **Chabrier '03**

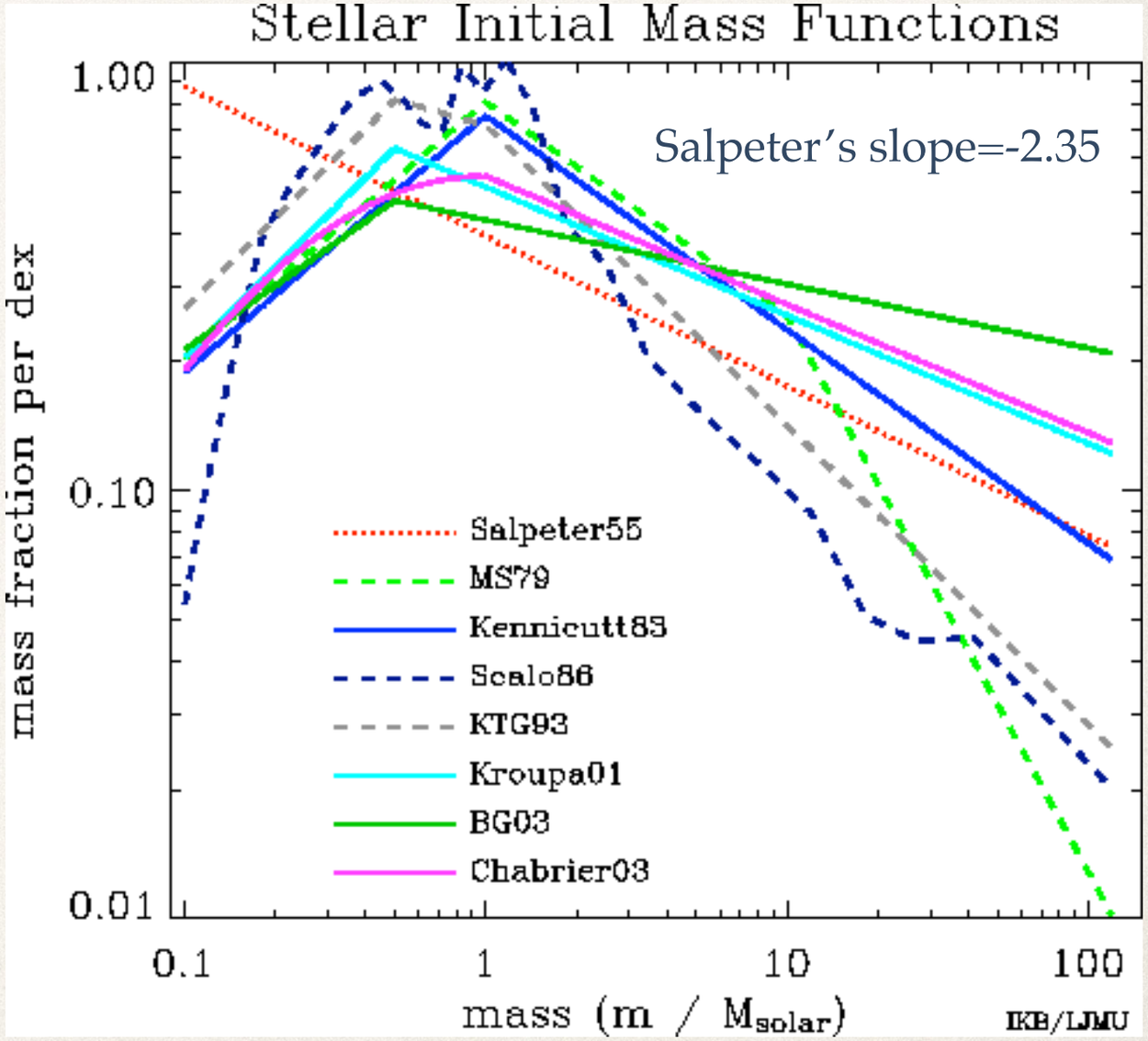

from Ivan Baldry's webpage

http://www.astro.ljmu.ac.uk/~ikb/research/imf-use-in-cosmology.html

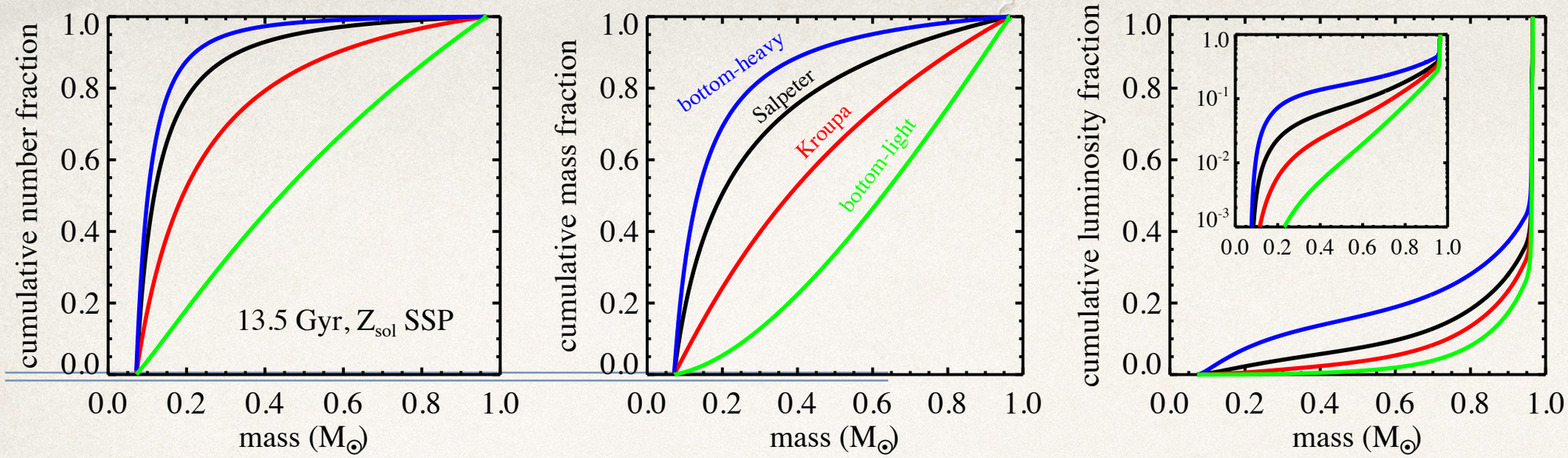

Conroy (2013)

Impact of IMF variations

- Always affect M/L normalization
- Different slope around TO affect color and luminosity evolution
- Most of current debate about
  - high mass end (≳20 $M_\odot$)
  - low mass end (<1 $M_\odot$)
- Almost a factor 1.8 in M/L from bottom heavy (eg Salpeter) to bottom light (eg Chabrier) IMF

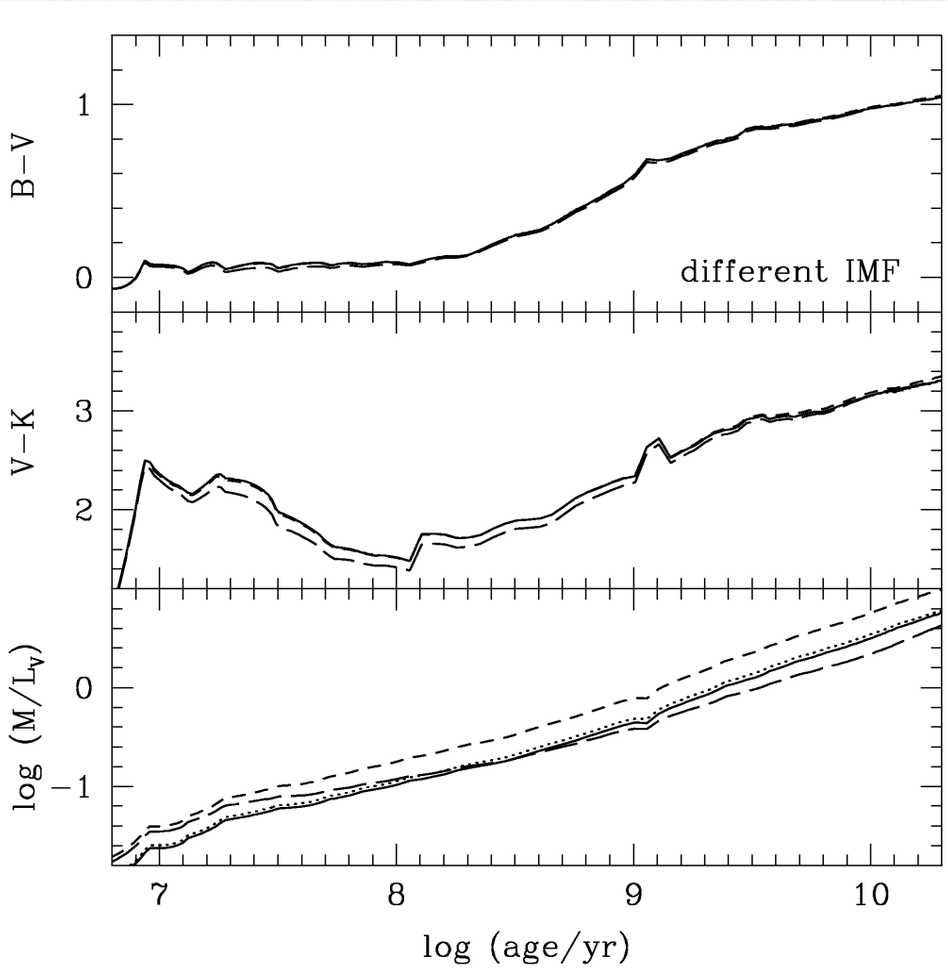

Figure 4. Evolution of the $B-V$ and $V-K$ colours and stellar mass-to-light ratio M/L_V of simple stellar populations of solar metallicity computed using the Padova 1994 stellar evolution prescription and the STELIB/BaSeL 3.1 spectral calibration, for different IMFs: Chabrier (2003b, standard model; solid line; see equation 2), Kroupa (2001, dotted line), Salpeter (1955, short-dashed line) and Scalo (1998, long-dashed line). All IMFs are truncated at 0.1 and 100 $M_\odot$.

Bruzual & Charlot (2003)

Effects of spatial resolution

- Galaxies (in general) are far from homogeneous

- Young and non-attenuated stellar populations tend to outshine the older and more attenuated ones

- This biases most of the inferences from global observables

- A lot to learn from spatial variations of stellar populations inside galaxies: when and how did stars in different regions form?

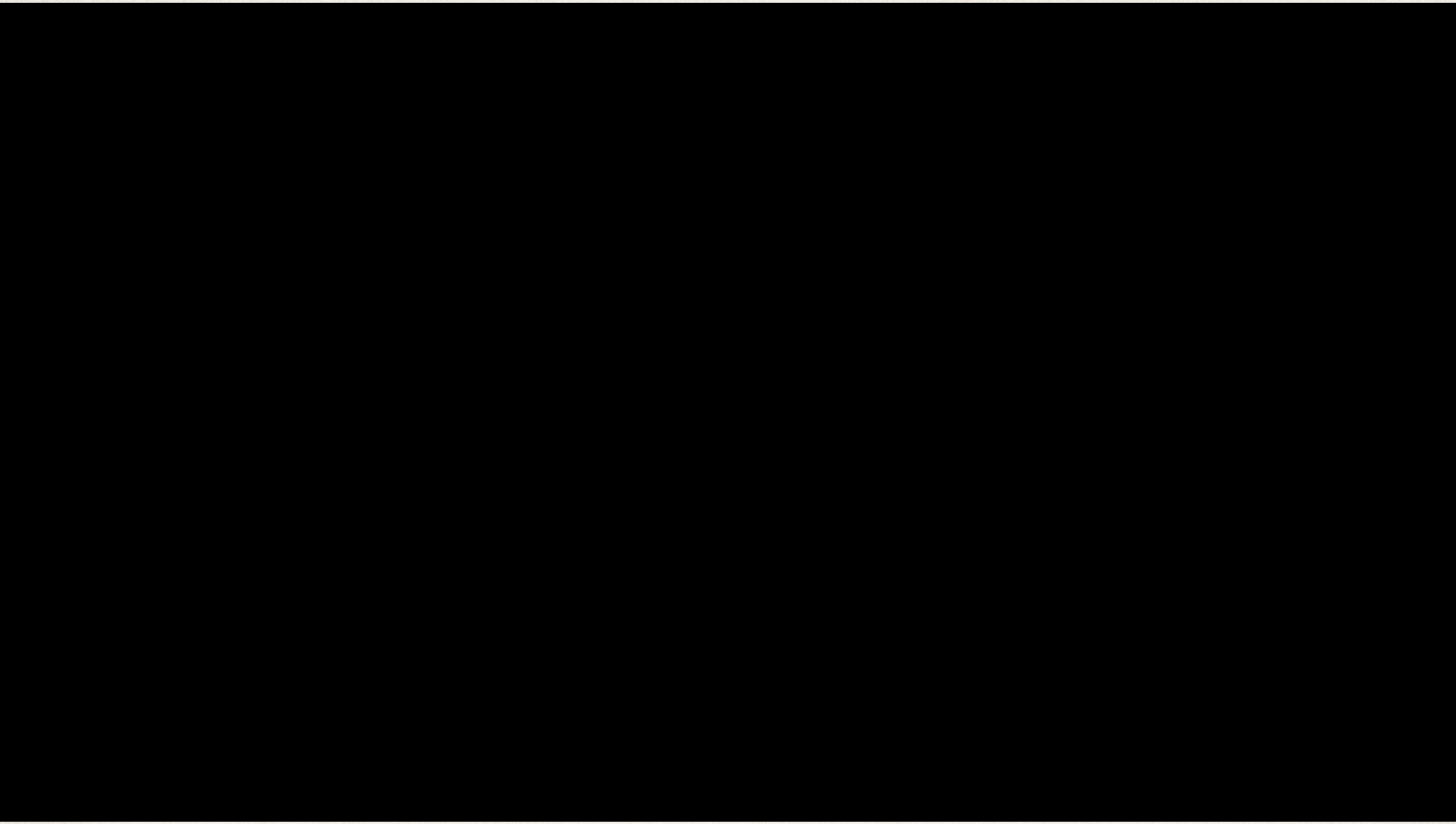

This view shows how the new MUSE instrument on ESO's Very Large Telescope gives a three-dimensional depiction of a distant galaxy. For each part of the galaxy the light has been split up into its component colours — revealing not only the motions of different parts of the galaxy but also clues to its chemical composition and other properties. This picture is based on data on the polar ring galaxy NGC 4650A that were obtained soon after the instrument achieved first light in early 2014.

Credit:
ESO/MUSE consortium/R. Bacon/L. Calçada

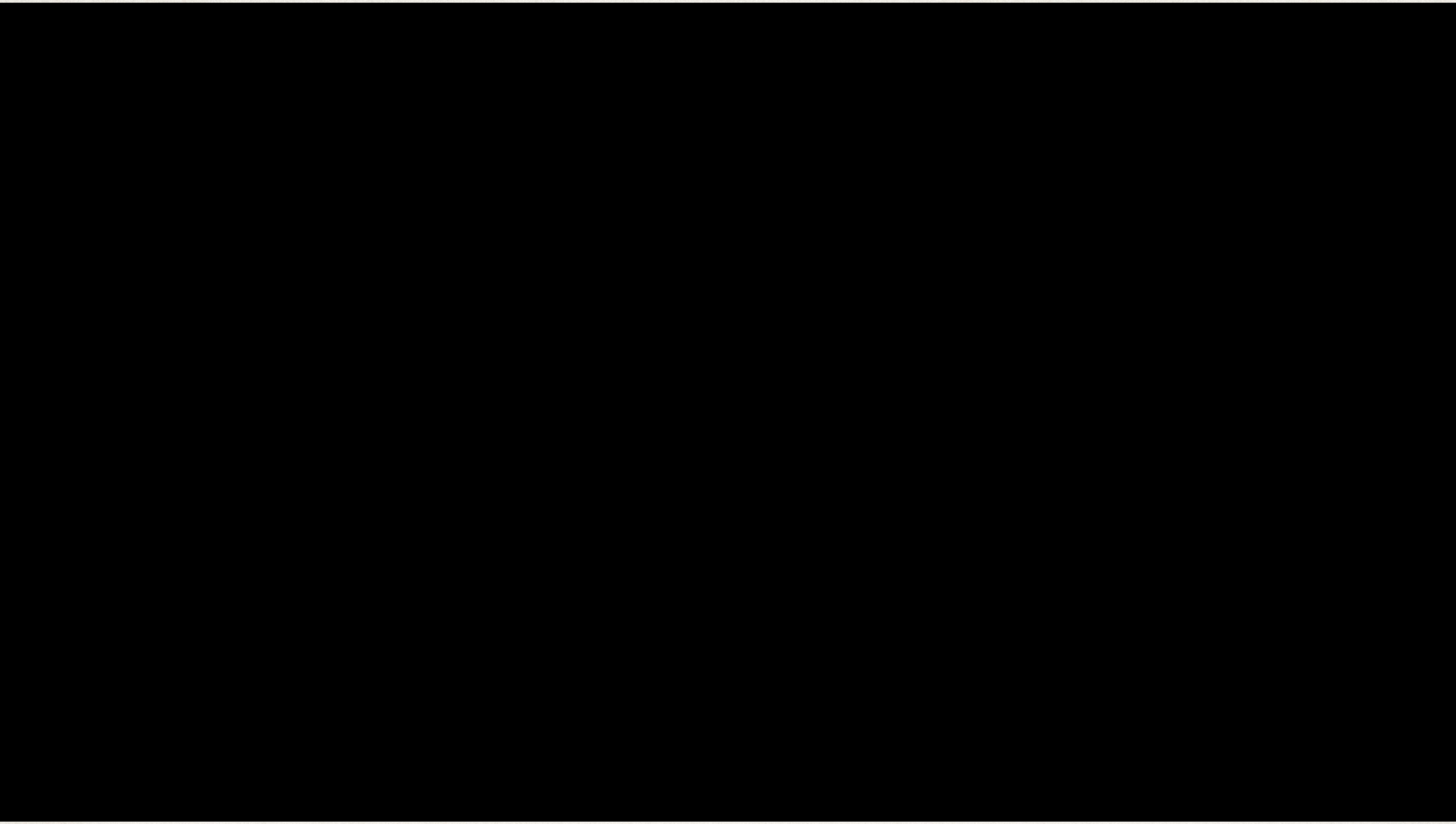

This view shows how the new MUSE instrument on ESO's Very Large Telescope gives a three-dimensional depiction of a distant galaxy. For each part of the galaxy the light has been split up into its component colours — revealing not only the motions of different parts of the galaxy but also clues to its chemical composition and other properties. This picture is based on data on the polar ring galaxy NGC 4650A that were obtained soon after the instrument achieved first light in early 2014.

Credit:
ESO/MUSE consortium/R. Bacon/L. Calçada

Integral Field Spectroscopy

- Analyze galaxies piece by piece!
- Calar Alto Legacy Integral FieldArea Survey (CALIFA): 600 galaxies
- MaNGA-SDSS: 10,000 galaxies
- SAMI (AAO): 3,000 galaxies

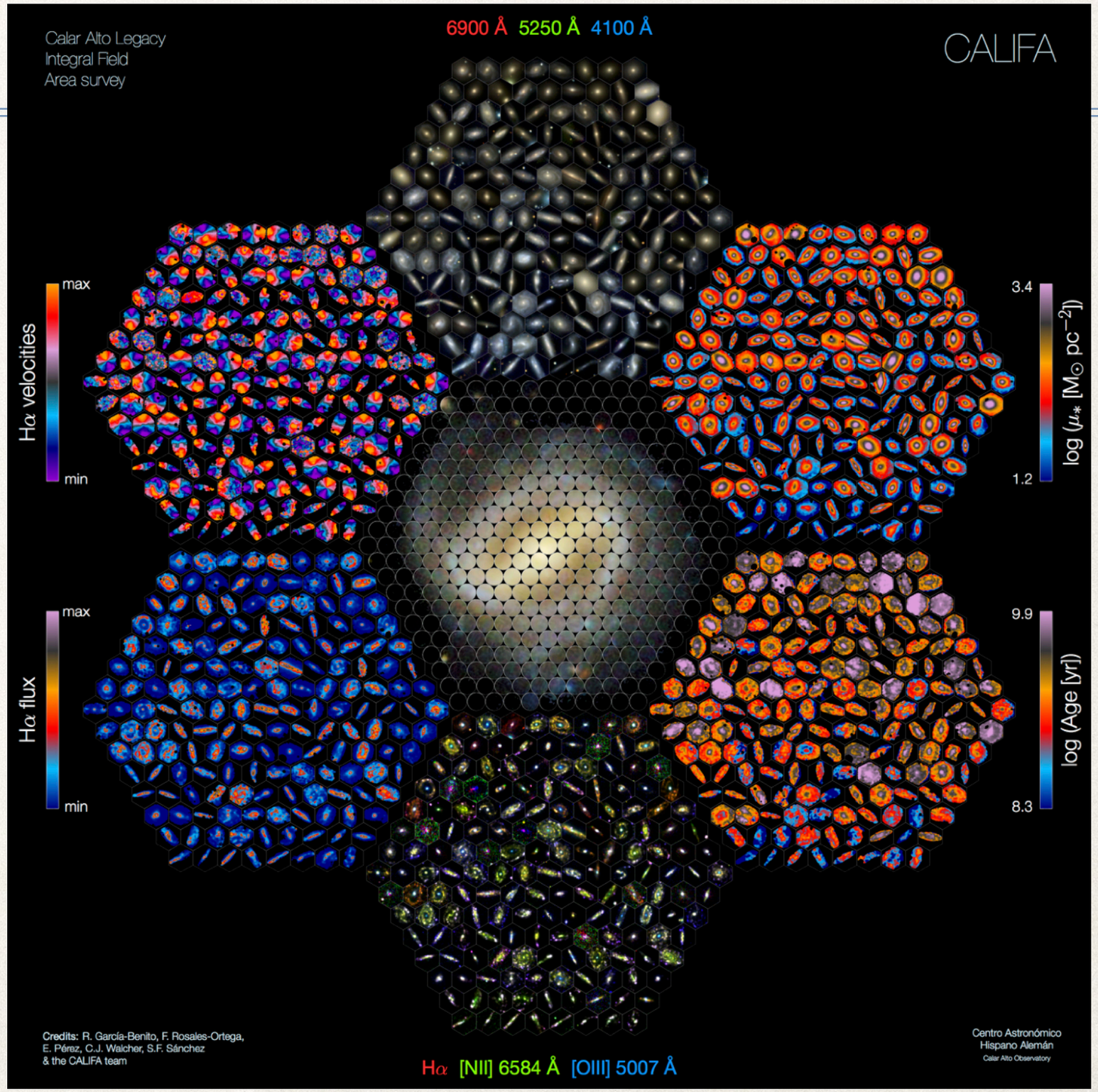

Diversity inside galaxies

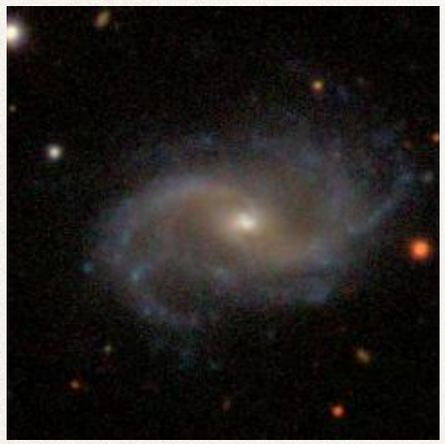

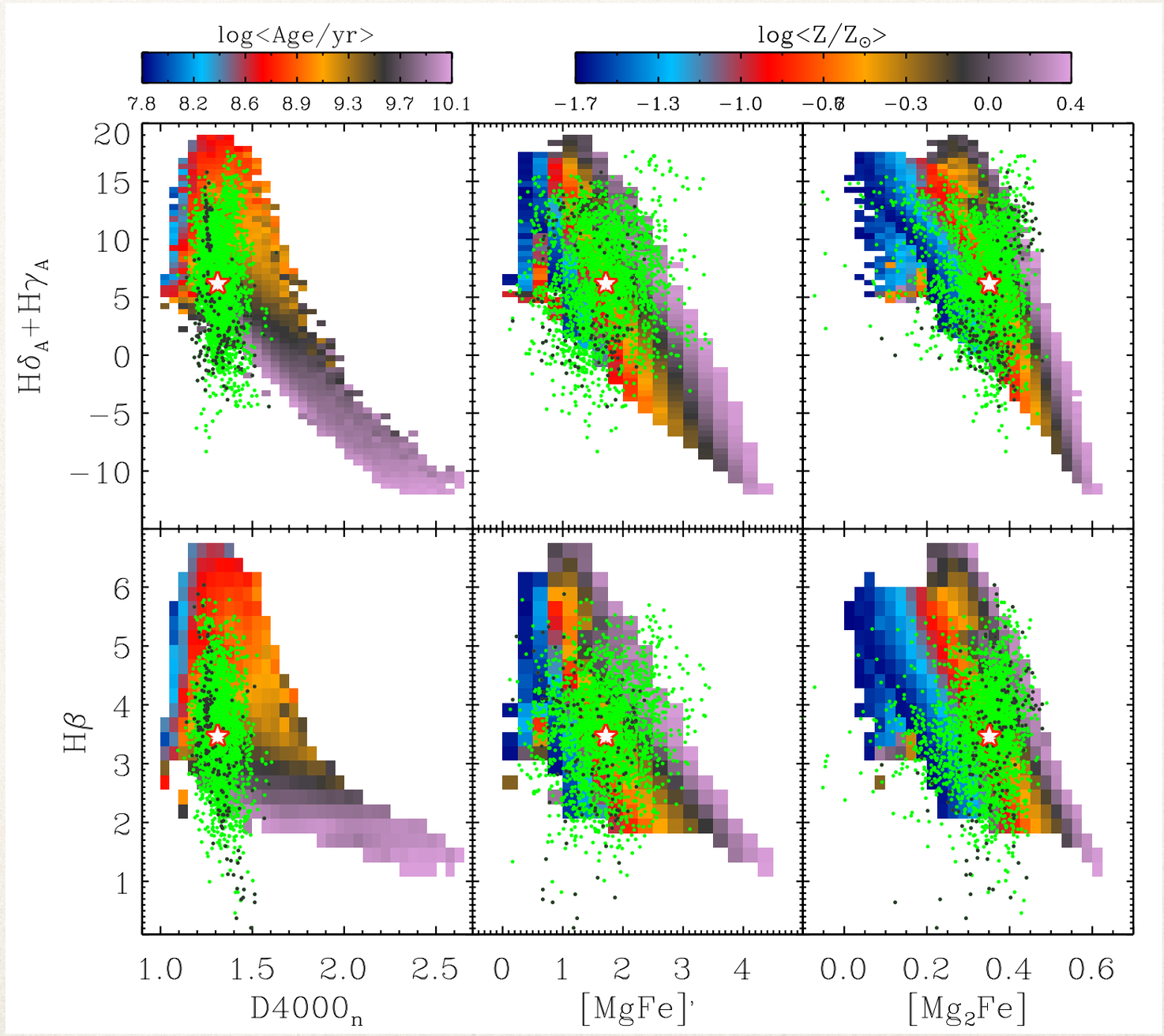

Diversity inside galaxies

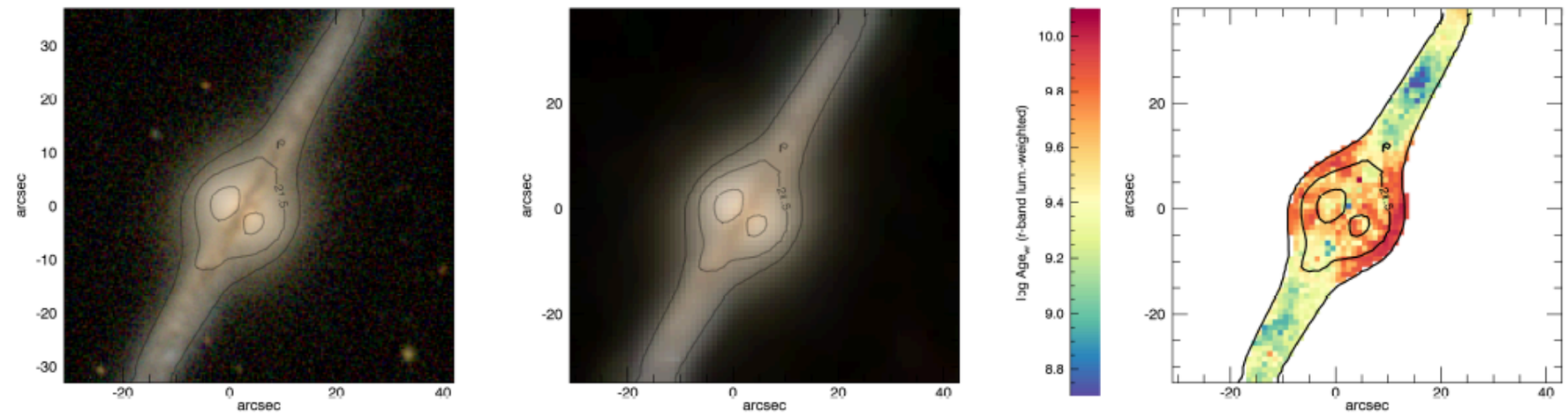

Figure 4. Example of a Sab spiral galaxy, UGC 10043, clearly displaying the age bimodality originating from the presence of a disc (young) and a bulge (old), emphasized by the edge-on view. The left panel is a *gri* color-composite SDSS image at the original resolution ($\sim 1.2''$), the central panel is the same *gri* color-composite degraded to the CALIFA resolution $\sim 2.6''$, and the right panel is the *r*-band luminosity weighted age map. *r*-band isophotes are drawn at 20.5, 21.5 (labeled) and 22.5 mag arcsec^{-2}.

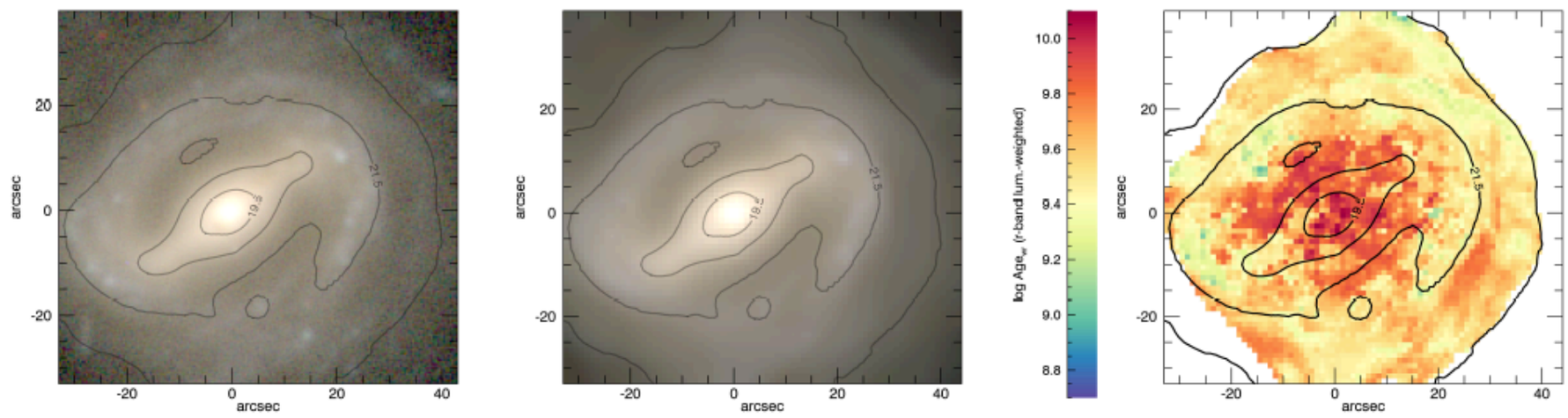

Figure 5. Example of a SBb spiral galaxy, NGC 0171, displaying that age bimodality at low surface brightness originates from the contrast of spiral arms characterized by young stellar populations and interarm regions where stars are substantially older. As in Fig. 4, the left panel is a *gri* color-composite SDSS image at the original resolution ($\sim 1.2''$), the central panel is the same *gri* color-composite degraded to the CALIFA resolution $\sim 2.6''$, and the right panel is the *r*-band luminosity weighted age map. *r*-band isophotes are drawn at 19.5 (labeled), 20.5, 21.5 (labeled) and 22.5 mag arcsec^{-2}

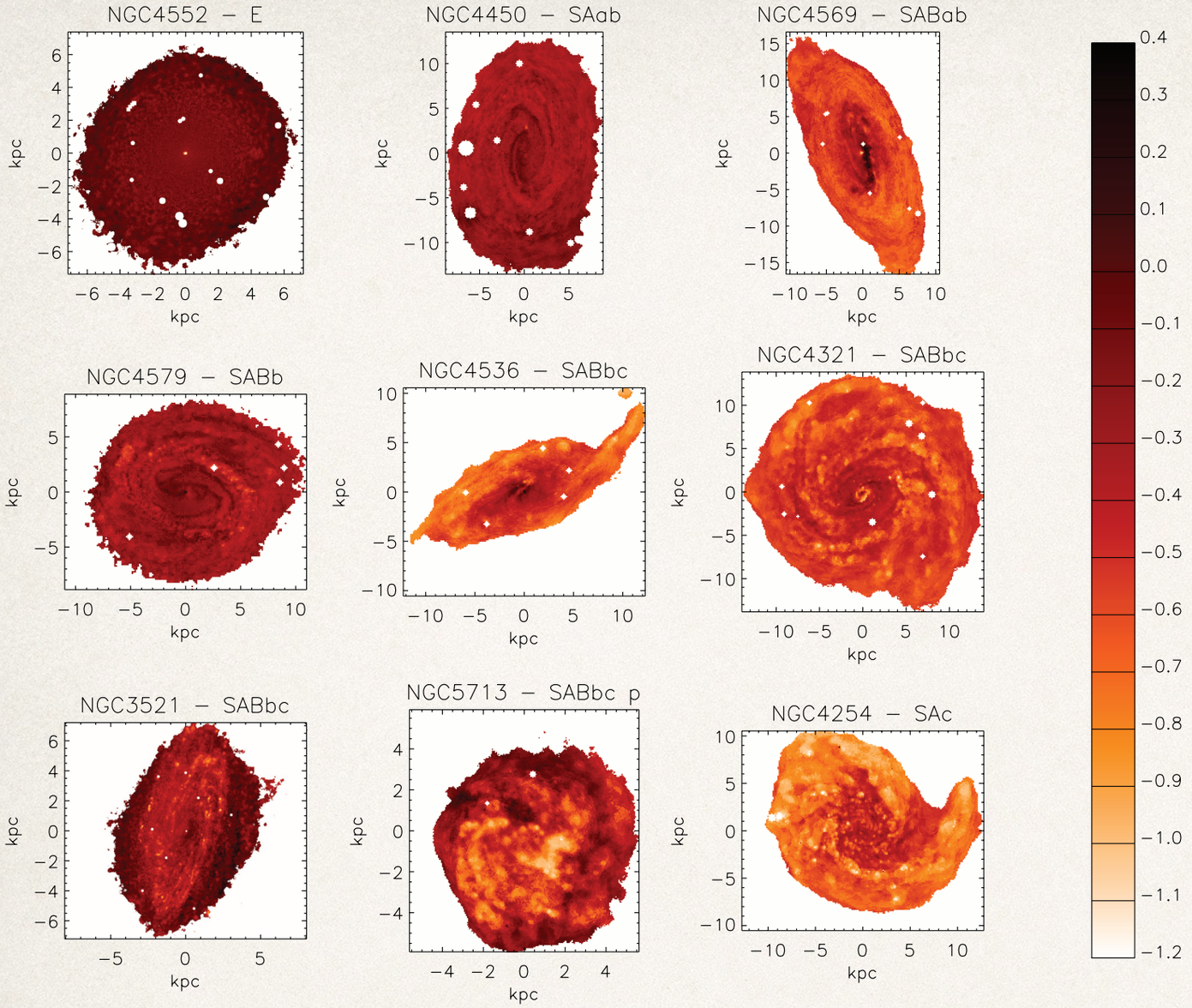

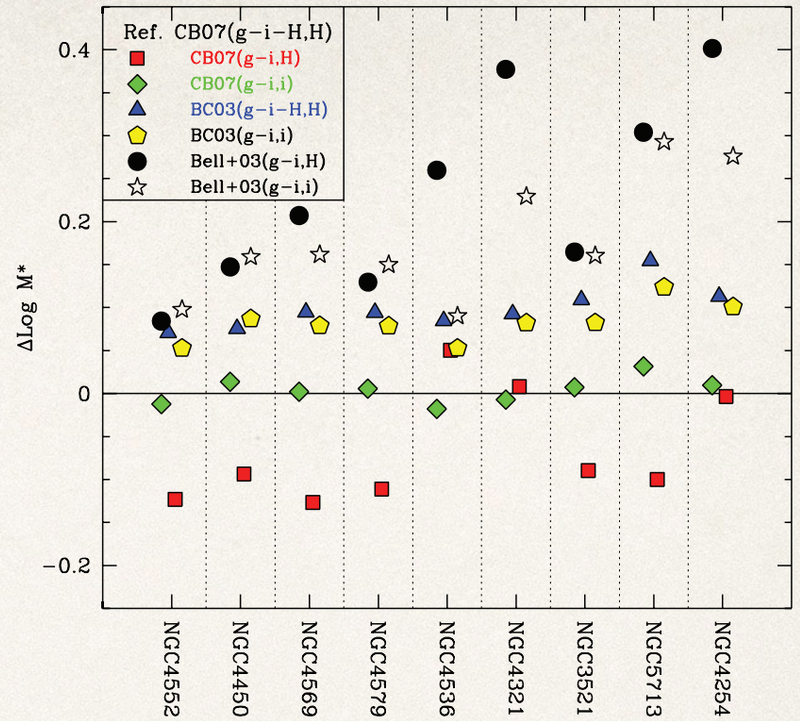

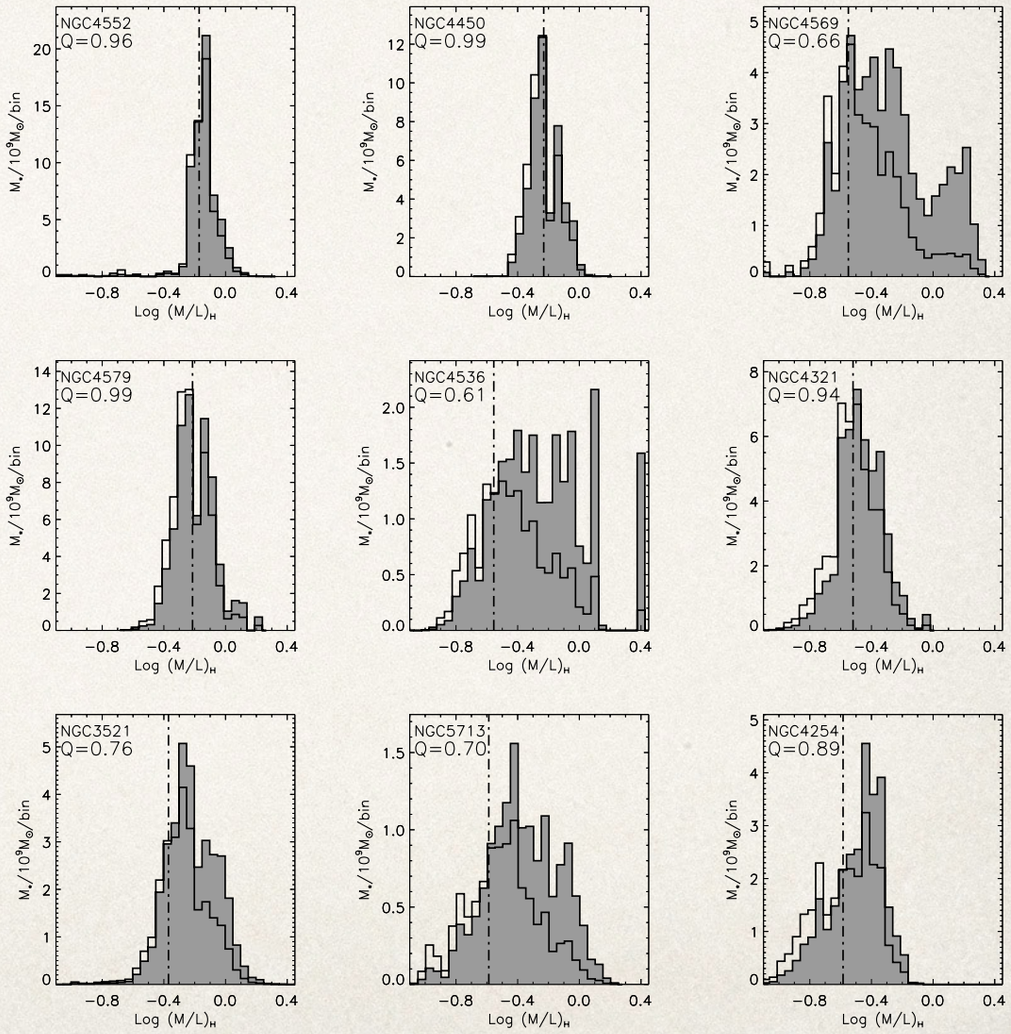

Zibetti, Charlot & Rix (2009)

MASS

LIGHT

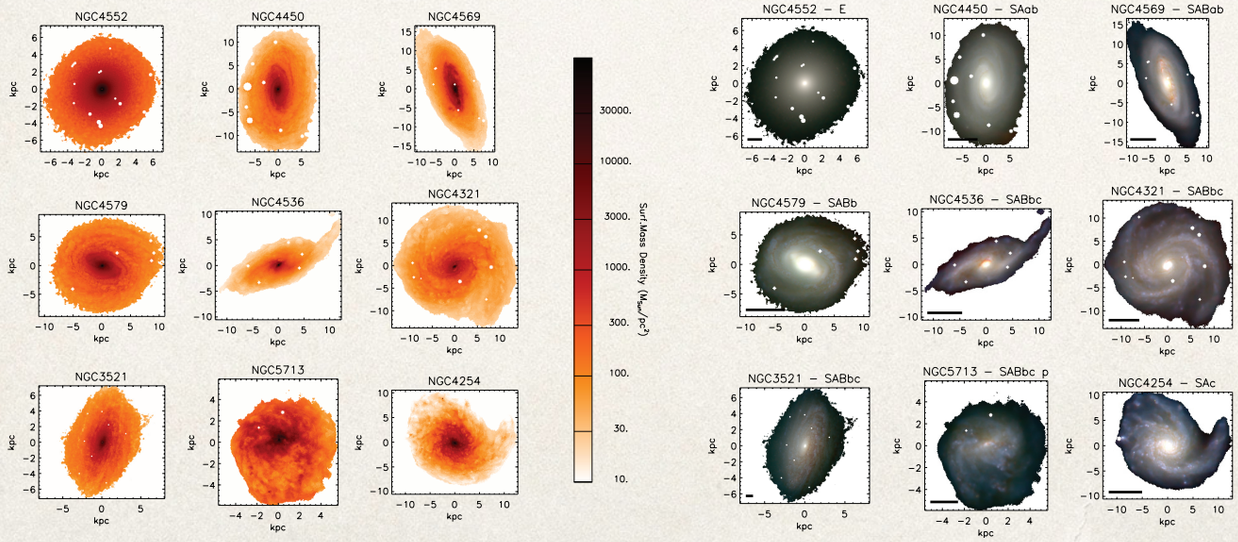

Shall we go red?

- Red and NIR can be very troublesome for the interpretation
  - uncertainties in models (see TP-AGB controversy)
  - optical already encodes most of the info
- HOWEVER much less biased in presence of
  - very young populations (see e.g. morphology in different bands!)
  - DUST! nothing to do if light does not come out

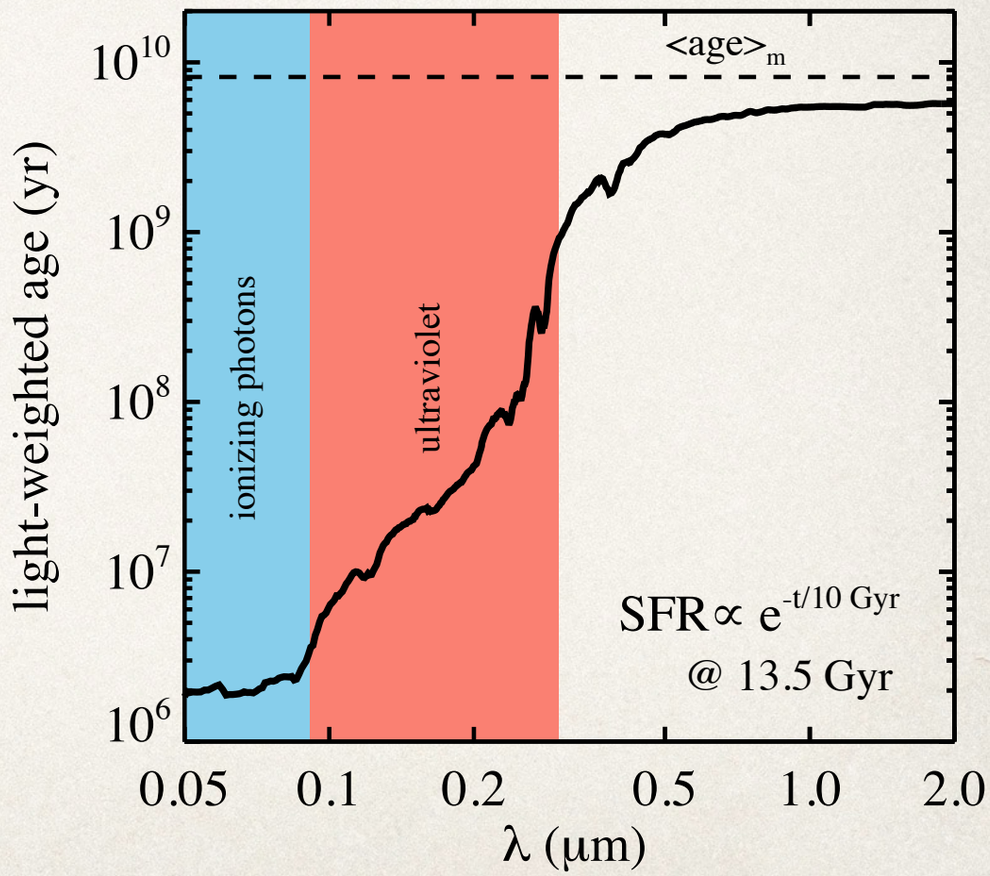

Conroy (2013)

TP-AGB stars and their impact on galaxy SEDs

late stage of the AGB phase for low- and intermediate-mass stars ($M \lesssim 5–7\ M_\odot$)
culminates in stellar populations of ages between 0.5 and 1.5 Gyr.

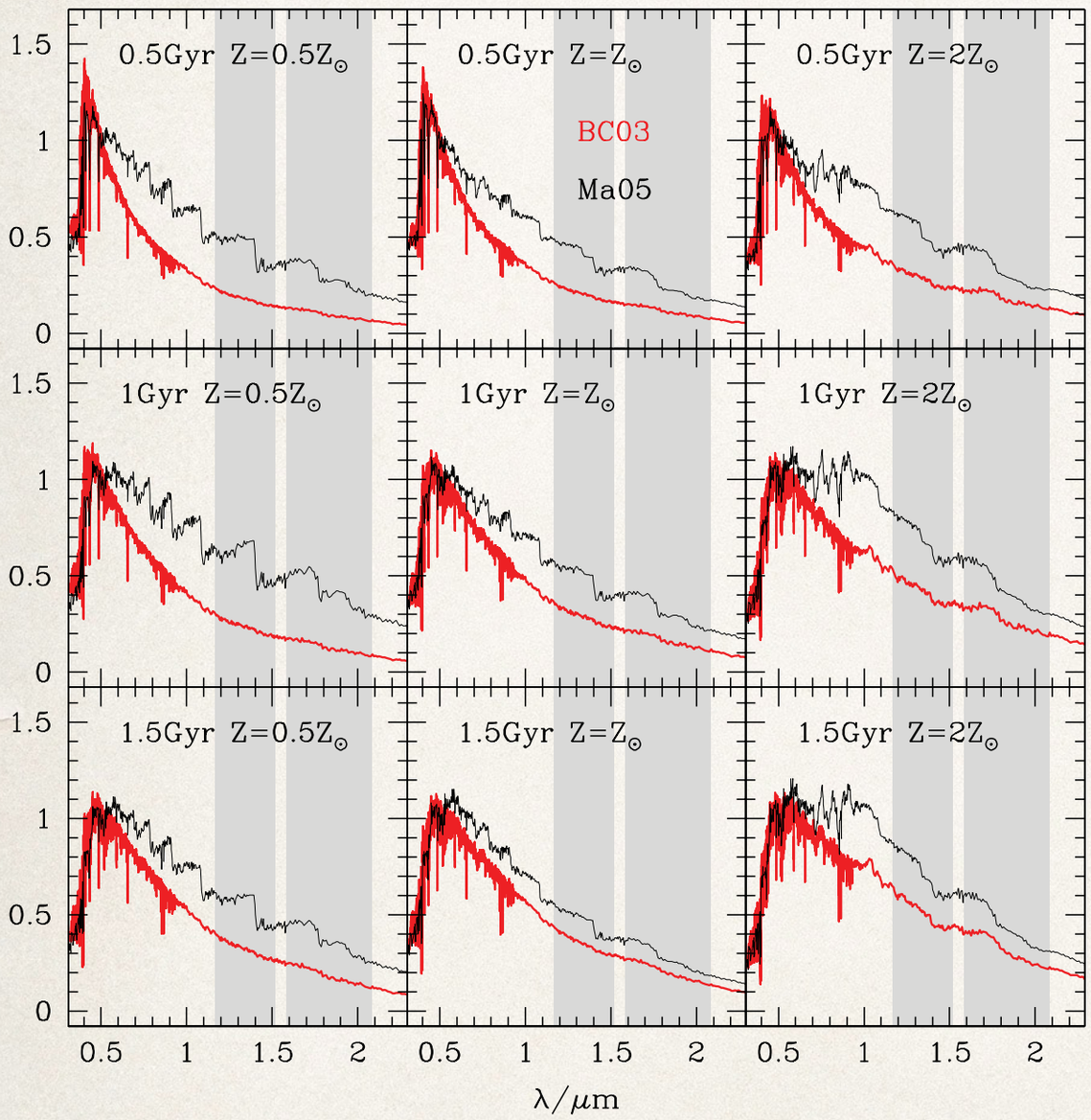

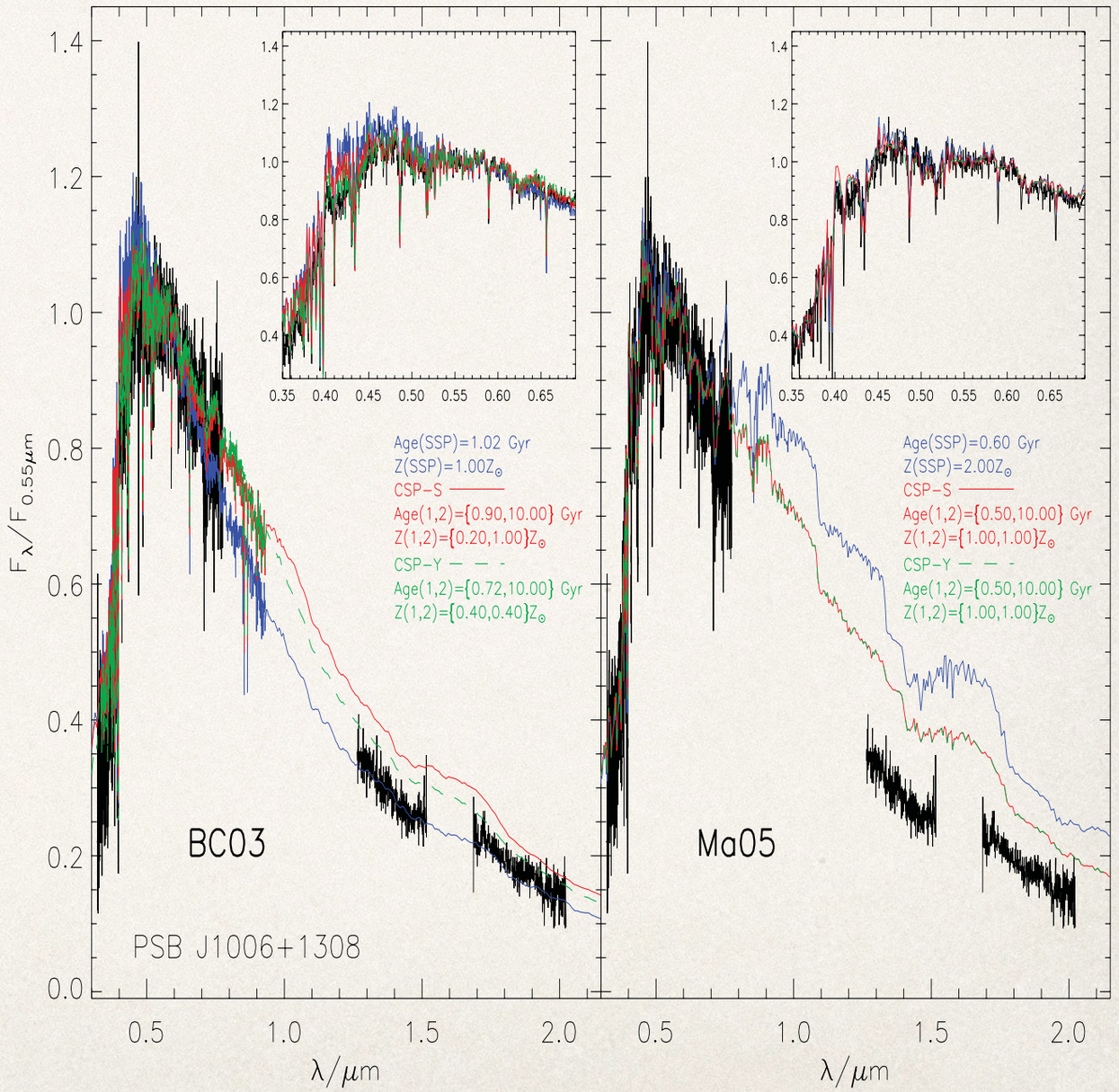

Zibetti et al. (2013)

SPS models and codes

Stellar population models predicting full spectra:

- Fioc and Rocca-Volmerange (1997, **PEGASE**)
- Bressan, Granato, and Silva (1998, used in GRASIL)
- Leitherer *et al.* (1999) and Vázquez *et al.* (2007) (both **Starburst99**)
- Vazdekis (1999, 2015, 2016)
- Schulz *et al.* (2002)
- Cerviño, Mas-Hesse, and Kunth (2002)
- Robert *et al.* (2003)
- Bruzual and Charlot (2003, **GALAXEV, or BC03**)
- Le Borgne *et al.* (2004, **PEGASE-HR**)
- Maraston (2005, **M05**, based on fuel consumption theorem)
- Lançon *et al.* (2008)
- Mollá, García-Vargas, and Bressan (2009)

Fully theoretical stellar population models:

- González Delgado *et al.* (2005)
- Coelho *et al.* (2007)
- …